ABSTRACT

TYAGI, SHREEYA. Correlate Protein Binding Capacity and Fiber Diameter of PBT Meltblown Substrates to Control Protein Adsorption. (Under the direction of Dr. Behnam Pourdeyhimi).

This research is aimed at investigating the effect of fiber diameter on protein binding capacity of polyester (PBT) nonwoven substrates, that are activated with grafted polymer brush surface(GMA-DEA). The first phase of the research involved production of Polybutylene terephthalate (PBT) meltblown substrates with varying fiber diameter distributions. These substrates were then characterized to evaluate process-structure-property relationship. Production parameters of higher melt throughput and reduced air velocity led to increase in mean fiber diameter. Tensile studies showed increase in peak load (lbf) for substrates with smaller mean fiber diameter suggesting better fiber-fiber interaction and web bonding.

The second phase of the research involved treating substrates with different fiber diameters with a coating of poly(glycidyl methacrylate) polyGMA through a UV grafting process in the presence of benzophenone as initiator. Further these grafted webs were treated with Diethylamine (DEA) to create an anion-exchange medium to test for equilibrium protein binding capacity. Characterization of these substrates post treatment was done through tensile testing, SEM, FTIR and weight gain. An increase in tensile strength was noted or all samples suggesting improved fiber-fiber interaction due to the coating. IR studies confirmed the presence of polyGMA and DEA on fiber surface.

During the third phase of the research, these substrates were characterized for equilibrium protein binding capacity, by exposing columns of PBT MB treated substrates to Bovine Serum Albumin (BSA).

It can be inferred that fiber diameter and pore size of the substrates have an effect on protein binding capacity and that due to the significantly reduced mass transfer resistances when treated nonwoven substrates were operated at high mobile phase flow rates, minimal losses in resolution was noted in case of some.

Correlate Protein Binding Capacity and Fiber Diameter of PBT Meltblown Substrates to Control Protein Adsorption

by
Shreeya Tyagi

A thesis submitted to the Graduate Faculty of
North Carolina State University
in partial fulfillment of the
requirements for the Degree of
Master of Science

College of Textiles

Raleigh, North Carolina

2011

APPROVED BY:

_____	_____
Dr. Ruben G. Carbonell Advisory Committee Member	Dr. Moon W. Suh Co-chair of Advisory Committee
_____	_____
Dr. Eunkyoung Shim Advisory Committee Member	Dr. Behnam Pourdeyhimi Chair of Advisory Committee

DEDICATION

To my most excellent mother

BIOGRAPHY

Shreeya Tyagi was born in Karnataka, India. She completed her Diploma in Textiles, from the National Institute of Design, Ahmedabad, India in 2006. After completing her postgraduate degree from Center for Technical Textiles, University of Leeds, United Kingdom in 2007 she came to the United States in Fall of 2008 to pursue a Master of Science degree in Textile, Apparel, Technology and Management at the College of Textiles North Carolina State University.

ACKNOWLEDGEMENTS

I am greatly indebted to my research advisor Dr. Behnam Pourdeyhimi, who provided me with a tremendous amount of guidance, motivation and above all, patience during the length of this research. I also wish to express my gratitude to my thesis committee Dr. Eunkyoung Shim, Dr. Ruben G. Carbonell and Dr. Moon W. Suh and for their advice and help during the course of this work.

It gives me great pleasure to thank all those people who played a critical role during the course of my Masters studies at NCSU. A special word of thanks to Dr.Yong Zheng, Dr. Amit Naik, Haiyan Liu and other members of Dr. Carbonell's lab in chemical engineering for their continuous help, since this research would not have been completed without their valuable input.

I would like to thank the NCRC Fiber Science Lab facilities for helping me manufacture the nonwovens and Dr. Carbonell's lab for providing the opportunity to pursue the current research. I want to express my very special appreciation for Mr. Stephen Sharp, Mr. William Barnes, Ms. Amy Minton and Ms. Teressa White from the College of Textiles for helping me through this process.

TABLE OF CONTENTS

LIST OF TABLES

LIST OF FIGURES

SECTION 1. INTRODUCTION

Chromatography (from Greek *chroma* ‘color’ and *graphein* ‘to write’) is the collective term for a set of laboratory techniques for the separation of mixtures, specifically, for the purification of proteins. It is regarded as the workhorse of downstream processing, providing high resolution for bioseparations. Isolation and purification of biotheraputic proteins are carried out using packed-bed chromatography columns, these columns are packed with high surface area porous resins which have ion exchange or affinity ligand functionalities (1) These high surface area resins exhibit diffusion limitations inside the particle pores and large pressure drops, low throughput and high production costs. ‘Chromatography alternatives’ that can replace traditional packed-bed are now being researched to reduce the extent of use of packed beds (2). Ion exchange membrane made of nonwoven fabrics display variable and controllable porosity since these fabrics can be produced with various fiber diameters and controlled poresize. Due to significant reduction in mass transfer resistance, treated nonwoven substrates can be operated at very high mobile phase flow rates with minimal losses in resolution. Throughputs achieved are much higher than those in packed beds resulting in shorter processing times, this further translates into, reduced product degradation (3). This research is dedicated to understanding the role of protein adsorption and how fiber diameters of treated nonwoven substrates are correlated. Poly(butylene terephthalate)PBT meltblown nonwoven substrates were activated with poly(glycidyl methacrylate) poly(GMA) and diethylamine(DEA) and tested for equilibrium protein binding capacity.

SECTION 2. LITERATURE REVIEW

2.1. Polybutylene Terephatalate (PBT) Properties (4)

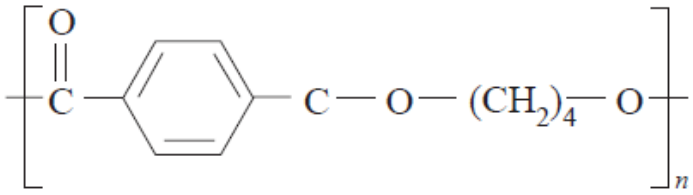

Figure 2-1. Structure of Polybutylene Terephthalate (5).

Polybutylene Terephthalate is a semi-crystalline engineering-grade thermoplastic, which is part of the polyester family of resins. It is a linear flexible aromatic polyester.

Table 2.1 Physical properties of PBT (4)

Physical properties	value
Density (kg/m^3)	**1310**
Tm ºC	**225**
Tg ºC	**60**

2.1.1. Hydrolytic degradation of PBT in extruder

PBT is hygroscopic and due to this reason drying of the resin prior to processing is critical to maintain property performance. Traces of moisture in the melt state degrades the intrinsic viscosity (IV) of the polymer, the IV of the polymer is a measure of molecular weight resulting in lower molecular weight. Moisture in the extruder causes a hydrolysis reaction between the polyester and water, lowering the molecular weight, strength and part toughness while increasing the meltflow (6).

PBT is usually dries to below 0.04% moisture at 121ºC for about 4 hours before processing. It has a relatively small processing window and during extrusion, the recommended melt temperature is between 243-266°C.

Table 2.2 Temperature guidelines for processing PBT (6)

Resin	Zone 1	Zone 2	Zone 3	Zone 4	Die	Melt Temp
PBT	232-243ºC	249-232ºC	254-266ºC	254-266ºC	254-266ºC	232-271ºC

2.1.2. UV degradation of PBT

UV degradation of polyesters is a well known phenomenon since polyesters are known to possess aromatic rings, these readily degrade on exposure to radiation >290nm.

Photolytic degradation or photo-oxidation can only occur when the polymer contains chromophores which absorb radiation wavelengths (>290nm) of the sunlight spectrum.

Chromophores present in the polymer can absorb radiation some of these are:

- Impurities present within the polymer chain.
- Polymerization catalyst residues, additives or pollutants, these are considered external impurities.
- Parts of the molecular structure of the polymer (i.e. aromatic rings in the case of PBT)
- Complexes that allow charge transfer between oxygen and the polymer chain.

When polymers degrade in the presence of radiation and air, the degradation mechanism is termed 'photo-oxidative' degradation. Photo-oxidative degradation is a faster process than when polymers are allowed to degrade under inert conditions. It is known for polyolefins that the photochemical degradation results in a series of oxidation products. While in the case of polymers which contain high amounts of chromophores, such as, the presence of aromatic rings in PBT, a profile of oxidation can also be attributed to the penetration depth of the radiation of wave lengths >290nm (7). PBT has a clear absorption of wavelengths >290 nm and due to this PBT photolysis and forms radicals which initiate oxidation reactions. Degradation of PBT in an inert atmosphere leads to the formation of CO and CO^2. It has also been noted that in the case of PBT fibers that UV degradation takes place to a certain depth of the material and this penetration depth depends on the length and type of exposure.

2.1.3. Alkali reaction on PBT

Alkali such as aqueous ethylamine is known to penetrate polyester and react initially in the amorphous regions of the fibers. Due to this reason, chain scission of polyesters occur, resulting in a considerable weight loss and the formation of hydroxyl and carboxyl end groups, weight loss in polyesters such as PBT would occur as terephthalic acid and butylene glycol are separated by the hydrolysis of the ester group in the polyester chains (8) .

Differences in reaction have been noted for NaOH and aminolysis, where it has been suggested that the reaction of polyester fiber with sodium hydroxide is topochemical and that aminolysis of polyester is a permanent reaction with preferential attack initially in the low-ordered regions of the fibers first. The weight loss in alkaline-hydrolyzed fabrics is proportional to the alkaline hydrolysis temperature, time, and the type of reagent (9).

2.2. MELTBLOWING PROCESS

During meltblowing, thermoplastic nonwoven fabric with microfibers are formed by a method where the extruded polymer melt is attenuated with hot air to produce stretched fibers that are driven along the air stream onto a collector surface (10).

In meltblowing the fundamental aspect is, a polymeric liquid jet (polymer melt) that is been stretched by high speed air flow (11). Air turbulences attenuate the filaments by stretching and breaking them down into finer fibers of varying length while at the same time transporting them to the collector, these fibers entangle in such a manner that it is impossible to remove one complete fiber from the web.

The extreme entanglement of fibers within the web contributes the strength to the web. Due to the attenuation of fibers with hot air, the fibers in the web have a fiber diameter distribution and the diameters of these fibers can range from less than 1µm to about 30µm. Web structures with fine fibers have very high intrinsic surface areas and these substrates can be used for filtration purposes (12) (13). The fiber arrangement in the web is not altogether randon due to the directional movement of the collector, hence the fibers tend to be more aligned in the machine direction (MD). However, the fibers in a MB web are overall largely isotropic.

The Die-to-Collector distance influences the fiber characteristics. The Die-to-Collector distance is defined as the distance between the polymer delivering orifice and the collector. The amount of time spent by fibers between the polymer delivering orifice and the collector influences the fiber orientation in the web, its strength and also surface properties. It can be noted that for fibers that spend a longer time in air , tend to produce weaker webs , this is due to the fact that , the attenuated fibers solidify before approaching the collector, resulting in minimum bonding among fibers.

It has been noted that process of attenuation takes place within approximately 200 microseconds and at short distances from the die (10-15cm). The force of the air attenuates the fiber from approximately 500µm diameter at the die orifice down to as small as 0.1 µm. This is a 5000 times reduction in the diameter of the fiber with 25 million times reduction in the cross-sectional area of the fiber (14).

For effective meltblowing of a polymer, the viscosity and the degree of polymerization of the polymer considered and used during the process is, usually lower than that used in the conventional melt spinning processes, this often leads to formation of weak or brittle webs. However in a case where the polymer IV is high an attempt to reduce the molecular weight of the polymer can be obtained through cracking or 'hydrolysis'.

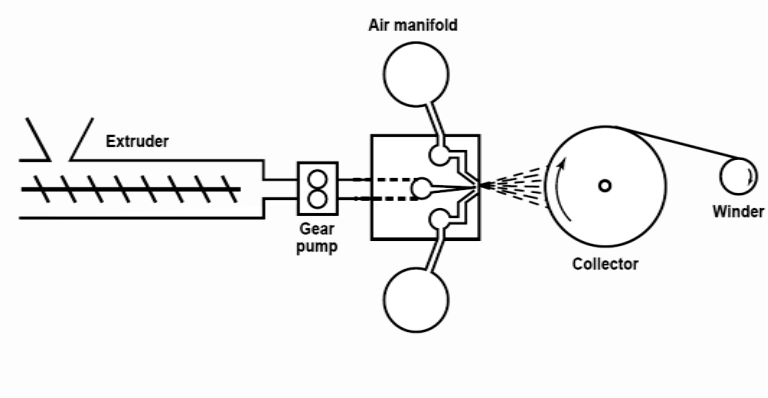

Figure 2-2. Schematic of a melt blowing process (15)**.**

During the meltblowing process the polymer in melt form is pushed through the extruder and introduced to a die containing multiple orifices. Streams of hot air converge and exit the die block assembly from either side of the die nosepiece, the turbulence produced attenuate melt forms fine diameter fibers that are finally collected on to the collector. A typical meltblowing (MB) equipment consists of an extruder, metering pump, die assembly, web formation, and winding.

2.2.1. Components of the Meltblowing Line

2.2.1.1. Extruder

The extruder is a heated barrel which is divided into different zone temperatures, the polymer pellets are introduced to the extruder by gravity feed, the screw conveyer which lies within the extruder carries the pellets and the polymer melt forward. As the polymer moves forward within the extruder, it melts, due to the heat, friction of the viscous flow and the mechanical action between the screw and the walls of the barrel.

As the polymer is carried forward within the extrude it is exposed to incrementally higher temperatures in the successive heating zones of the barrel, which causes it to melt further and reach the desired temperature. The screw and the barrel, is divided into feed, transition, and metering zones.

- In the feed zone the polymer pellets are preheated in a deep channel screw and pushed to the next zone.

- The screw in the transition zone has a decreasing depth channel that aids in the compression and homogenization of the melting polymer.

- In the metering zone maximum pressure is exerted on the melt in the forward direction. Impurities such as dirt , foreign particle and non-melted polymer lumps are removed during this phase.

2.2.1.2. Metering Pump

A metering pump is device that is responsible for positive displacement of a constant volume of polymer melt at set rate to the die assembly. The metering pump ensures consistent flow of clean polymer mix under process variations in viscosity, pressure and temperature. The polymer subsequently enters the ‘die’, which is heated to the desired melt blowing temperature.

2.2.1.3. Die Assembly

The die assembly has three distinct components and is heated to the desired meltblowing temperature. The three components of the die are:

- Polymer feed distribution
- Die nosepiece
- Air manifolds

The polymer feed distribution is responsible for the flow and the feed of polymer melt inside the block. The feed distribution specifically designed so that the polymer distribution is less dependent on the shear properties of the polymer since the die has no mechanical control over the variations in the polymer flow across the die width. The feed distribution balances both the polymer melt flow and its residence time across the width of the die (16).

The polymer melt goes from the feed distribution channel directly to the die nosepiece. The die nosepiece is made of metal , it is hollow and tapered with orifices across its width. The polymer melt is extruded from these orifices.

Hot air is forced through the air manifolds of the die, which finally flows through the gas slots and attenuates the filament strands to form fine fibers. A typical die nosepiece has aprox.(0.1-0.4 mm) diameter orifices spaced at 25 to 100 per inch. The capillary and drilled hole type are the two of the die pieces to be used (17).

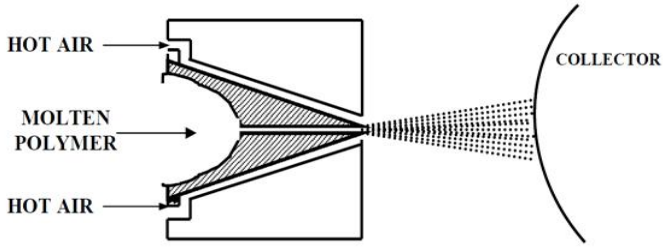

Figure 2-3. Schematic of the die assembly and web collection (15)**.**

2.2.2. EFFECTS OF AIR VELOCITY AND THROUGHPUT ON WEB FORMATION AND FIBER DIAMETER OF MELTBLOWN SUBSTRATES

The process parameters (15) that would be varied include:

- Polymer throughput
- Attenuating air pressure
- Die to collector distance

2.2.2.1. Polymer Throughput

Polymer throughput is a major factor that affects the fiber diameter and web characteristic. As the melt throughput increases the fibers that are formed would have a larger diameter

where as in the case of lower melt throughput the fibers that are formed in comparison would have a smaller mean diameter.

2.2.2.2. Attenuating Air Pressure

The attenuating air that exists the die block breaks the melt polymer stream into fibers stretching them and carrying them to the collecting surface. The higher the attenuating air the finer will be the fibers**,** however the final diameter also depends on the melt throughput and die-to-collector distance.

2.2.2.3. Die to Collector Distance

The die to collector distance (DCD) determines the morphological development of the polymer melt. If the distance is very close, the fibers are not fully formed and "shot" could be formed. Also the basis weight will be affected at close ranges as the high temperature attenuating air stream will "rebound" and width of the web formed will be affected.

2.3. FILTRATION

'A filter medium is any material that under the operating conditions of the filter is permeable to one or more components of a mixture, solution or suspension and is impermeable to the remaining components' (18).

A filter is a device which allows separation to be achieved among the components of a suspension or solution, where the suspension or solution may be in gas, liquid or solid phase.

A filter medium, often referred to as a membrane or a thin sheet of natural or synthetic material that is permeable to substances in suspension or solution, while being able to retain the other desired components. The retained components may be in the form of solid particles, colloidal material, proteins and molecular or ionic species. Further it can be said that, through a filter medium, separation may occur by the means of electrical, mechanical, chemical and physical forces. In the case of an ion-exchange membrane, surface charge is employed as a mean of protein capture. Membrane chromatography is when you have microfilters that have absorption properties. Versus sieving and filtration, where there's no absorption.

2.3.1. Filtration Mechanism: Depth filtration

When the desired component to be captured is much smaller than the poresize of the filter material such that component/particle capture is not due to sieving mechanism, then most theories in particle capture are to do with depth filtration (19).

- **Inertial impaction**: Particle inertia overcomes air streamlines and impacts fiber surface.
- **Interception:** Particle is intercepted by the fiber surface and this is described as a point in time 't' where the distance between particle and the fiber surface is less than or equal to the radius of the particle's center of mass. The mechanism of interception is that the particle is carried to the fiber surface through along the streamline and then it attaches itself to the fiber surface.

- **Molecular diffusion:** Brownian motion of particles, this method of trapping particles is based on the probabilistic motion of particles to vary from the streamline and attaches itself to a fiber.
- **Charge:** Electrostatic forces can be retained temporarily on the surface of fibers and are especially effective against dust particles. However, surface charge on the fiber surface can also be created through surface activated coatings, as in the case of ion-exchange membranes where protein adsorption on the treated fiber surface is due to charge.

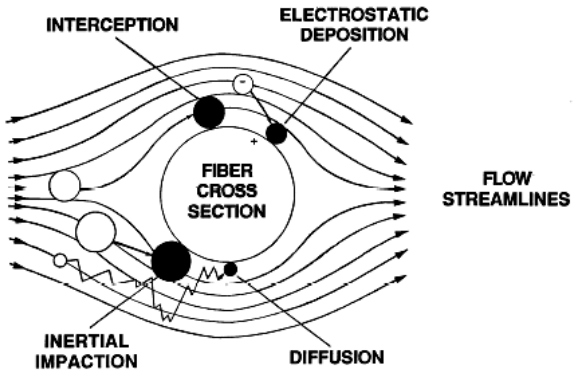

Figure 2-4. Filtration mechanism utilized in depth filtration (20)**.**

2.3.2. Filtration of Aerosol Particle

The mechanical filtration of aerosols was proposed by Irving Langmuir during World War II defined theories on aerosol filtration. His theory on filtration of Aerosol's concentrated on spherical aerosol particles of less than 1µm diameter that avoid gravitational effects, linear

face velocities of less than 3.5cm/s and inertial effect of filtration. Through the study of Langmuir's theory, Ramskill & Anderson (21) developed concepts which also involved looking at inertial effect as a contributing factor to the total effective penetration %. However they considered direct interception as a factor devoid of the influence of linear velocity.

(MPPS) Most penetrating particle size: 0.04 - 0.4 microns (40-400 nanometers) Particles that are of size between 0.04-0.4 microns, these have been said to have too small mass to illustrate inertial impaction and too large for diffusion and have been termed difficult to capture (21).

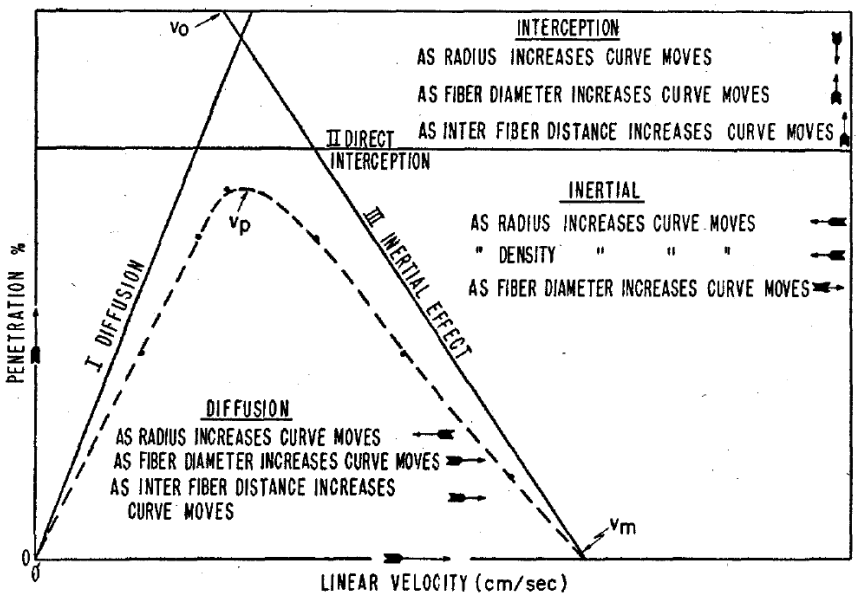

Figure 2-5. Demonstrating filtration mechanisms at work considering substrates fiber diameters and radius , it is expected that the inertial mechanism should become measurable at some velocity (vo) and should exert no additional effect above some velocity (vm), (vp) is velocity at maximum particle penetration (21)**.**

The MPPS are also velocity related and will decrease in size as the velocity increases. For a small particle size there is also a velocity of maximum penetration. Hence for or a given filter was there should be a particle size difficult to filter than most.

According to Ramskill & Anderson et. al. (21) 'diffusion factor' worked at lower fluid velocities while 'direct interception' took over at fluid velocities above the range where 'diffusion' is active, this was however not affected by the fluid velocity gradient and would be active till a point where inertial effect kicks in at a certain velocity. The inertial effect lasts till the velocity of the fluid is high enough to counteract the inertial force of the particle.

Also according to this model, particle size is kept constant and the fluid velocity is gradient. So, it gives a picture of how the filter medium would function under various fluid velocities and what the maximum penetration velocity for that particular particle size would be.

A fixed volume of fluid will only flow with a linear velocity through fixed points in space with only a constant interaction limit with each point, this would not change if the velocity of fluid changes, only the number of particle with each interaction point would increase or decrease per unit time, however the interactions will be of a fixed number. This is a constraint that would hold true only while considering linear velocity and constant streamlines. However, even with a constant velocity, inside the nonwoven filter media streamlines would change and would be dependent on web structure.

Spurny et. al. has considered inertial effect and direct interception together and so, he does not consider interception independent of fluid velocity. His model shows how a filter medium would function at capture of various particle sizes and states that the MPPS would vary with fluid velocity.

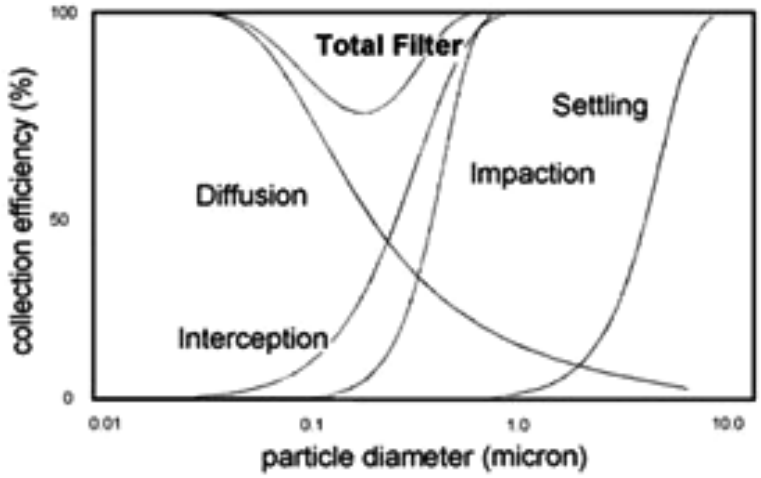

Figure 2-6. Typical fraction collection efficiency curve for filter media (22)**.**

Nonwoven can be defined as a sheet, web, or mat of natural and/or man-made fibers or filaments excluding paper, that have not been converted into yarns, and that are bonded to each other by any of several means (INDA 1999).

Nonwoven filters are classified either neutral or electrostatic filters, here we only consider neutral fibrous filters that have been treated to produce ion-exchange membranes to be used for chromatography purposes. These substrates are assemblies of fine fibers, and fiber diameter are normally smaller than 50μm. with random orientation distributions with a polymer brush coating.

Detailed work in protein separations using ion-exchange membranes have been conducted by Etzel et. al. where BSA was separated from dilute solution using an ion-exchanger with an average pore size of 150μm were performed at three different flow-rates of 0.2, 1.0 and 5.0 ml/min.

It was noted that for 150µm pore sized membrane that there was a strong dependence on the flow-rate due to the overall system dynamics were not at equilibrium. At low flow-rates, the behavior of the system behavior indicated ideal flow. With reduced pore size and reduced flow-rate cauesd an increase in the protein diffusion coefficient, causing increase in the efficiency of the membrane.

The performance of ion-exchange membrane systems are greatly influenced by key parameters such as flow-rate, average pore size and solute diffusion coefficient.

It has also been observed in previous works where no flow-rate effects were observed because the membrane pore size was too small, however in the case of large pore sized membranes, what happens is that due to the pores become large the protein flows through the membrane faster than it has time to bind by adsorption mechanism, since it needs to diffuse to the wall of the membrane and bind before it passes through (23) .

2.4. POLYMER BRUSH SYSTEM AND THEIR POTENTIAL APPLICATION IN BIOSEPARATION

2.4.1. What are polymer brushes ?

Macromolecular assemblies that are chemically tethered at one end to a substrate. The special physical properties of polymer brushes arise from the covalent attaching of the polymer chains to the solid substrate. As in the case of PBT MB microfibers these can be exposed to GMA (Glycidyl Methacrylate) and through UV polymerization GMA grafted polymer brushes are obtained on the surface of the fibers.

The concept of polymer brushes as a protein adsorbing surface originated from the development of Self-Assembled Monolayers (SAMs).

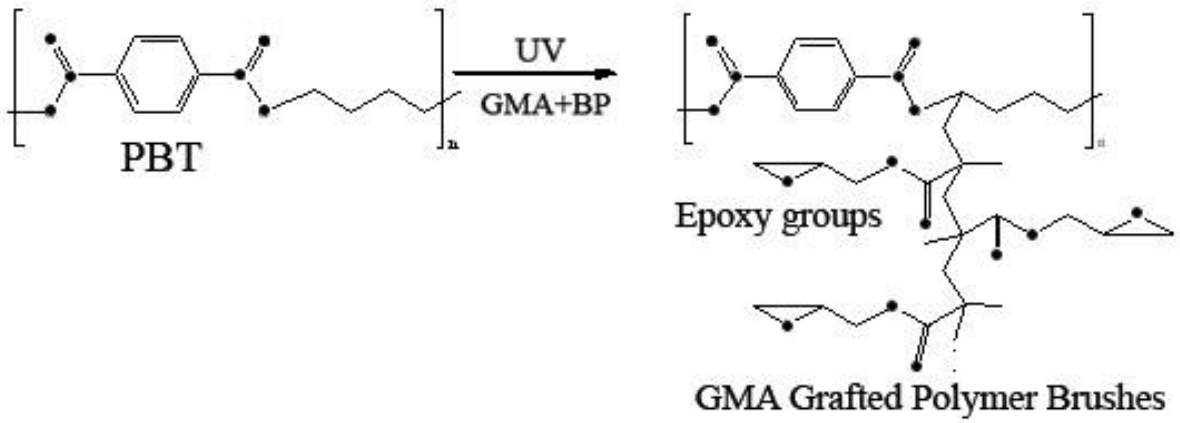

Figure 2-7. Grafting of PBT with Glycidyl Methacrylate (GMA) (3) (24)**.**

SAMs have been employed to modify and custom the surface chemistry of metals, metal oxides and semiconductors in a large way. SAMs is composed of a 'mainhead-group', with a special affinity/attraction for the substrate, the mainhead-group is attached to a 'functional group' through the medium of a 'main chain' (25).

The limitations of SAMs is that due to the self-assembling nature of their formation, although large monolayer free of defect can be obtained mono-layers are only several nanometers thick and are mechanically fragile.

Table 2.3 Comparison of SAM and polymer brush system (26)

SAMs	Polymer Brushes
Long chains of aliphatic molecules are fully extended to maximize packing density and van der Waals interactions. (27)	For polymer brush chains to extend and remain in their stretched conformation would demand huge entropic cost, hence a disorder at the molecular level is noted.
An assembly of small molecules	Mono-layers of macromolecules
Upright chains	At low grafting density, the so-called "mushroom" regime the polymers adapts more or less random coil conformation.
Nanometers	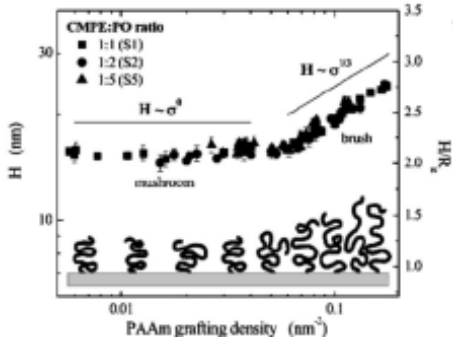 Wet thickness of Polyacrylamide (PAAm) as a function of the PAAm grafting density. Above a cartoon illustrating different polymer states with increasing grafting density.

'The conformation of polymer brushes is regarded a conventional problem and the degree to which chains are stretched away from the surface is determined by the competition between the entropic energy loss due to chain stretching and the excluded volume interactions between different segments of the brush' (25). In a good solvent the brush height is predicted to be defined by the degree of polymerization (N) and in a poor solvent the scaling is $N^{1/3}$.

2.4.2. Methods of Preparation of Polymer Brushes

Polymer brushes are deposited or grafted on substrate surfaces through three commonly used techniques, namely, spin coating, Langmuir-Blodgett-Kuhn technique and SIP technique. These have been illustrated in Figure 2.8

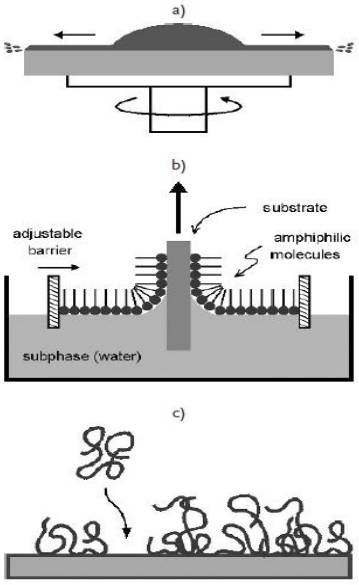

Figure 2-8. Different processes used for the deposition of polymers on surfaces: (a) spin-coating (b) Langmuir-Blodgett-Kuhn (LBK) technique (c) SIP technique adsorption from solution (26)**.**

2.4.3. Surface-Attached Polymers

To control interaction of a material with its environment, surface-initiated polymerization (SIP) reactions is a method for the preparation of functional coatings. This technique is based on the growth of polymer molecules at the surface of a substrate from surface-bound initiators (26).

End of the polymer chains can be held on the surface by:

- Physisorption
- Covalent Bonding

When the grafting density is very high, the polymer chains are forced to adopt a conformation where the single chains overlap and because of this, the polymer chains strongly move away, stretching from the substrate and achieve a shape which is very different to the typical random coil conformation that polymer molecules adopt in solution. Such covalently attached chains, that compose a film like surface on the substrate have strongly stretched chains are called ‘polymer brushes’.

Accordingly, very obvious differences that can be observed in the behavior of free coils and that of polymer brushes is, especially noticed, in the case where polymer chains require shearing and stretching. An example of such a situation would be, while molecules are penetrating the polymer brush surface from solution due to adsorption, since, polymer brush surfaces are often used as to capture molecules such as protein from solution.

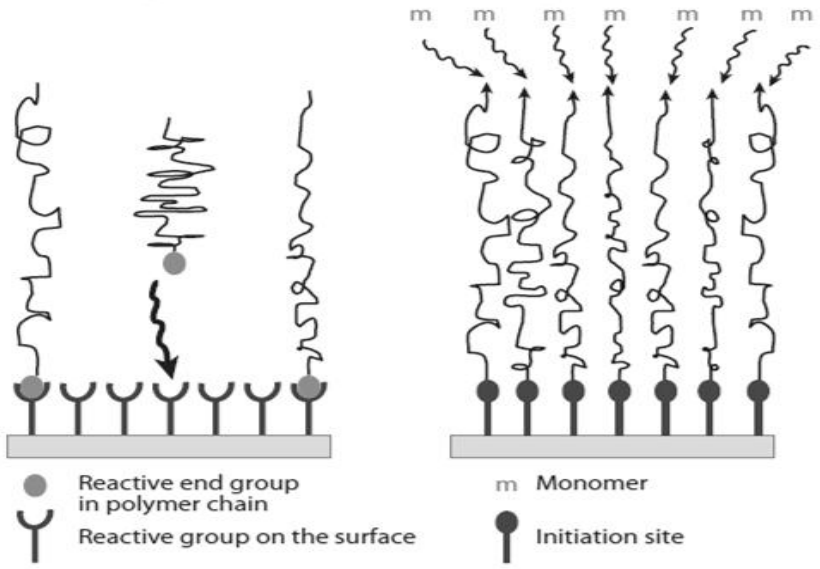

Figure 2-9. Polymer brush approach 'grafting to'(right) vs. 'grafting from'(left) SIP approach. The influence of grafting density and the enthalpic and entropic factor are clearly present in the 'grafting to' approach (28)**.**

During the 'Grafting to' approach, already formed polymer chains are attached to a substrate surface, in this case the polymer chain carries an 'anchor' group either as an end group or in a side chain. This anchor group is made to reacted with appropriate site-points on the substrate surface producing a surface-attached layer of polymer chains. In the case of side chain tethering leads to multiple points being attached at the same point and this result in a flat conformation of the polymer chains. Since, the chains do not have the freedom to stretch being covalently bound. The 'grafting to' also limits the polymer chain immobilization due to steric hinderance. Figure 2.9 demonstrating the 'grafting to' method.

In the case of ‘Grafting from’ polymerization reaction takes place in the presence of a substrate onto which monomers had been attached. During this process, a radical attacks a site-point on the surface of the substrate, in the second step, a monomers unit is added to that site-point, so that the chain gradually grows.

2.4.4. Polymer Brushes: General Features

As discussed in Section 2.4.3, it is possible to create a molecular ‘bottlebrush’ where polymers are attached as side chains to the backbone of a polymer molecule, in this research many poly(GMA) side chains is attached to the main chain poly(GMA) as described in Figure 2.10 so that, every segment of the backbone carries such a polymeric side chain.

Some general features of this sort of polymers, where chains attached to substrate surfaces at only one end can take on and two sort of chain conformation. These are the ‘mushroom’ conformation or the ‘brush’ conformation.

When polymer molecules are fixed to a substrate surface, two basic conformation cases can be observed, this depends on the grafting density of the chains:

1. If the distance between two polymer chain while they are tethered to a site-point on the substrate, is greater than the size of the attached polymer chains, then the individual chains act independently and behave in the manner of single chains attached to the substrate surface. In such a situation, according to the interaction of the polymer chain with the substrate surface energy, two chain conformation ideas can be observed.

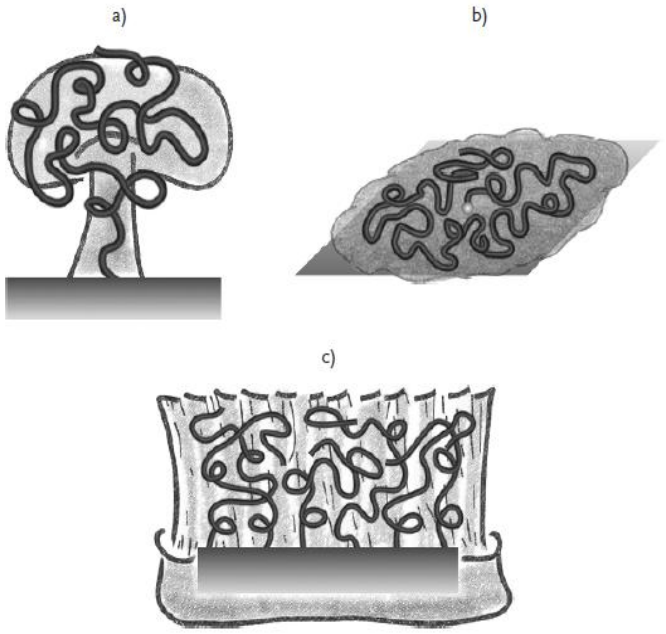

Figure 2-10. Polymer brushes (a)'mushroom'(b)'pancake'(c)'brush'conformation (26)

- If the influence of the polymer and the surface is repulsive, the chains form a a well known 'random coil' or 'mushroom' conformation. It can be observed that due to this the chains stretch away from the surface and is linked to the substrate only through a 'stem' of short length.
- However, if the polymer chain is strongly attracted to the substrate surface, then the polymer chain takes on a flat conformation.

2. In a case where polymer chains are attached to the surface at short distances between each consecutive chain then in such a case, the polymer molecules interact and are not indipendent. The polymer chains attempt to avoid each, other, causing them to stretch away from the substrate so as to minimize interaction among themselves.

This stretching of these polymer chains reduce the overall system energy, causing a point of reduced entropy, in the system. Thus, it can be said that, with the polymer chains in conformation of being stretched away from the substrate surface provide a new equilibrium at a higher energy.

*'The main idea behind the theoretical description of polymer brushes is that the free energy '**F'** of the chains is obtained from a balance between the interaction energy between the statistical segments '**Fint'** and energy difference between stretched and unstretched polymer chains '**Fe'** (elastic free energy) caused by the entropy loss of the chains'* (26)*:*

F = Fint + Fe…….(1)

2.4.5. Polyelectrolyte Brushes for Protein Adsorption

Brushes which carry charges along the polymer chain that interact specifically with ions in the surrounding medium and produce (local) changes in the solubility of the polymer, that plays a key role in describing the swelling behavior of these brushes are often referred to as 'polyelectrolyte brushes' (29). Figure 2.11 gives a simplistic view of a polyelectrolyte brushes system. It can be observed that the arrangement of charges in the chain affect the overall confirmation of the chains.

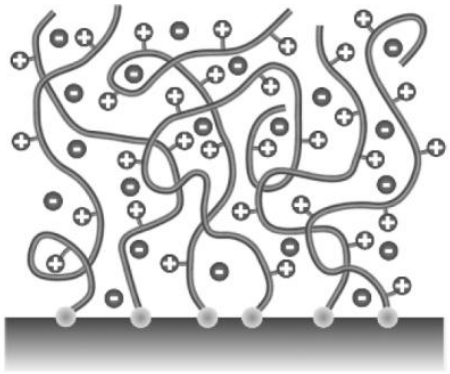

Figure 2-11. A simple description of a polyelectrolyte brush system (29)

Figure 2.11 describes Poly(GMA) brushes are grafted on PBT fiber surface and further treated with Diethyl amine (DEA) to create an anion-exchanger, this coating of GMA-DEA can be described as polyelectrolyte brushes when such a surface is surrounded in a medium with ions, hence the charge on the brush surface is temporary and active only in the case where ions are present in the surrounding medium.

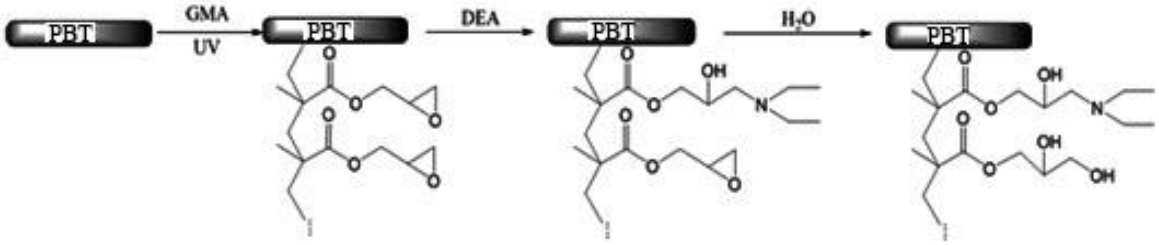

Figure 2-12. Ion exchange membrane from GMA Grafted PBT, uniform GMA grafts conversion of epoxy to DEA (diethylamine), conversion of the remaining epoxy to diol (3) (30)**.**

2.4.6. Protein Adsorption Mechanism

Certain interface properties that can be controlled by the application of a thin organic film on the surface of a substrate, these properties are, friction, adsorption of molecules from the surrounding or to avoid nonspecific adsorption of proteins, hydrophobicity and hydrophilicity or wetting with other liquids, interfacial localization of terminal groups diffusion control, regulation of steric repulsive forces control of phase-segregation in response to external stimuli lubrication and flocculation control (31).

Proteins are known to adsorb on to various surfaces via a number of non-specific and specific interactions including, van der Walls interactions, electrostatic forces, hydrophobic forces and hydrogen bonding (32).

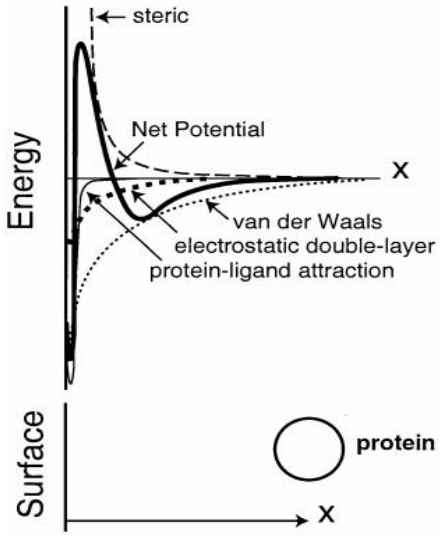

Figure 2-13. Forces in play while describing interaction between soluble protein and a surface. The net potential profile in solid bold line is a superposition of the van der Waals potential which is the dotted line, the attractive and repulsive double layer potential (bold dashed line), steric repulsion (long dashed line) and specific, short range interaction (solid line) (32)**.**

Polymer brush systems can be used to regulate interactions that include interactions of the substrate with liquids, solids, particles, proteins, cells, etc.

The effect of the grafting density of brushes can be generalized:

- Van der Waals interactions may strongly dominate, when in the case, at low grafting of polymer brushes, molecules such as proteins, can easily diffuse through the brush system and reach the substrate surface.

- As the grafting density of the polymer brushes improves and when the brush is exposed to a good solvent, repulsive forces in the system may dominate creating a resistance to protein adsorption.

- A situation where grafting density is very high, a rise in attractive forces is observed.

Optimum grafting densities can be explained in a manner where, for a moderately grafted substrate it can be considered that, small particles would interact strongly with the polymer brush, this would then allow the particles to disperse freely within the brush system while the big aggregates would be expelled towards the brush-air interface.

While at a very high grafting density where attractive forces within the brush system are at play, the particles will be expelled from the brush, giving rise to the concept of protection material (31).

2.5. BOVINE SERUM ALBUMIN (BSA) (33)

Physical properties of BSA:

- Number of amino acid residues: 607
- Molecular weight: 66.399 kDa
- Isoelectric point in water at 25 °C: 4.7 above this point at pH 7.4, the protein net charge is negative, an important consideration for anion exchange chromatography.
- Extinction coeffecient of 0.667 $mg^{-1}cm^{-1}$ at 279 nm
- Dimensions: 140 X 40 X 40 $Å^3$ (prolate ellipsoid where a = b < c)

Proteins such a Bovine Serum Albumin (BSA) can have a positive or negative charge depending of the pH, at the 'isoelectric point' this charge is neutral. At pH 7.4 BSA is above its PI and possesses a negative charge.

2.5.1. BSA Adsorption (34)

2.5.1.1 pH dependence

In various studies conducted on BSA adsorption regarding polymeric surfaces it has been noted that a certain pH the adsorption is maximum, while at other pH values there is least absorbance. This can be attributed to the fact that BSA is folded best at its pI (4.7) and at a value higher ~pH 7.4 or a value lower ~pH 2.2 this is not the case.

At the pH of 2.2 it is more acidic than the iso-electric point of BSA (pI 4.7) and at the pH

value 4.3 is near the pI of BSA, whereas the pH 7.4 is more basic than the pI. It has been observed that at the pI of BSA (pH 4.3), a greater amount of BSA was noted to be adsorbed and it reached its maximum value, with a decrease, in the case of the lower and higher pH values.

The maximum amount adsorbed protein can be related to BSA conformation, where it is observed that at its pI the protein is more folded than at any other pH. At a pH value greater or smaller than the pI, the protein adsorption dropped a great deal. This can be explaned through the electrostatic repulsion between BSA molecules, since they tend to have the same charge, i.e. +ve at pH 2.2 and -ve at 7.4. As observed, the UV spectra of BSA show differences under different pH conditions. This indicates that BSA conformations depend on the pH. At a pH values higher than the pI, BSA appears to be –ve charged, whereas it is +ve charged at pH values lower than the pI. The UV absorbance at pH 7.4 relates to the negative charge of BSA conformations, and the UV absorbance at pH 2.2 is due to the positive charge of the conformations.

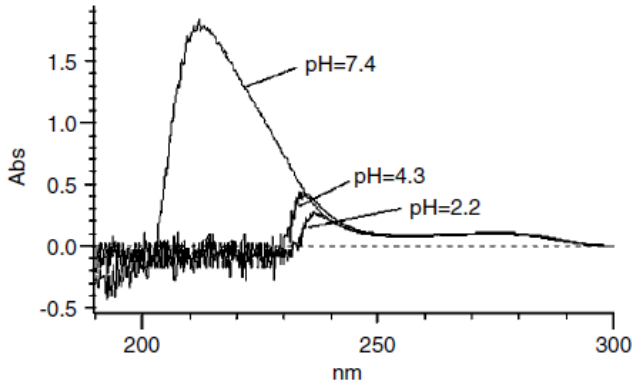

Figure 2-14. UV spectra of BSA at various pH conditions (34)**.**

2.5.1.2. Ionic strength dependence

Concentrations of salts such as NaCl also have an effect on BSA adsorbance, in the case of ion-exchange chromatography, Na and Cl are often used as ‘counter-ions’. In a study regarding sulfonated microspheres as the matrix, it was noted that at pH 2.2, the presence of NaCl (0.025-0.1M) increases the amount of BSA adsorbed on to the anionic surface. The increase is evidenced by the increase in NaCl concentration. However, at pH 4.3, close to the pI of the protein, the amount adsorbed appears to decrease in the presence of NaCl (0.025-0.1M), indicating that the effect of NaCl on BSA adsorption is closely associated with pH. The greater adsorption with the increase of sodium chloride conc. at pH 2.2 could be held as the reason for the reduction of the electric double-layer of BSA. Due to the presence of NaCl, decreases the repulsion among adsorbed BSA protein molecules and thus increases the adsorption has been noted. However it has been observed that, at pH 4.3, close to the pI of the protein, BSA protein can have a conformation that is more folded, which can affect the adsorption. Also, the binding of Cl and BSA at this pH can obviously decrease the amount of protein adsorbed.

2.6. ION-EXCHANGE CHROMATOGRAPHY

Purification of proteins can be based on their structural properties, where each technique uses a specific single parameter (e.g. charge or hydrophobicity) to effect adsorption and separation, this is different from separation based on biological interaction. Chromatography can be defined as the differential separation of sample components between a mobile phase and stationary phase (35).

2.6.1. Ion Exchange Chromatography

Ion exchange chromatography is considered an extremely important and popular technique for the purification of proteins and various other charged molecules. Positively charged molecules are captured using –vely charged functionalities on the surface of beads, this is known as cation exchange chromatography. Conversely, in anion exchange chromatography negatively charged molecules are attracted to positively charged functionalities that are attached on the stationary phase (i.e. porous beads, treated membranes or nonwoven substrates).

2.6.1.1. Mechanism

So that all charged molecules bind well, the mobile phase is that is considered is a low to medium conductivity (i.e. low to medium salt concentration i.e. PBS pH 7.4) solution. The adsorption of proteins on to the functionalities present on the stationary phase is driven by the ionic interaction between the oppositely charged ionic species/functionalities on the protein surface and in the functional groups on the stationary phase.

The strength of the interaction between the protein/species is governed by the number and location of the charges on the protein surface and those provide by the functional group. By increasing the salt concentration the proteins with the weakest ionic interactions start to elute from the column. Proteins that have a stronger ionic interaction with the stationary phase require a higher salt concentration and elute later. Hence, binding capacities of ion exchange resins are usually quite high.

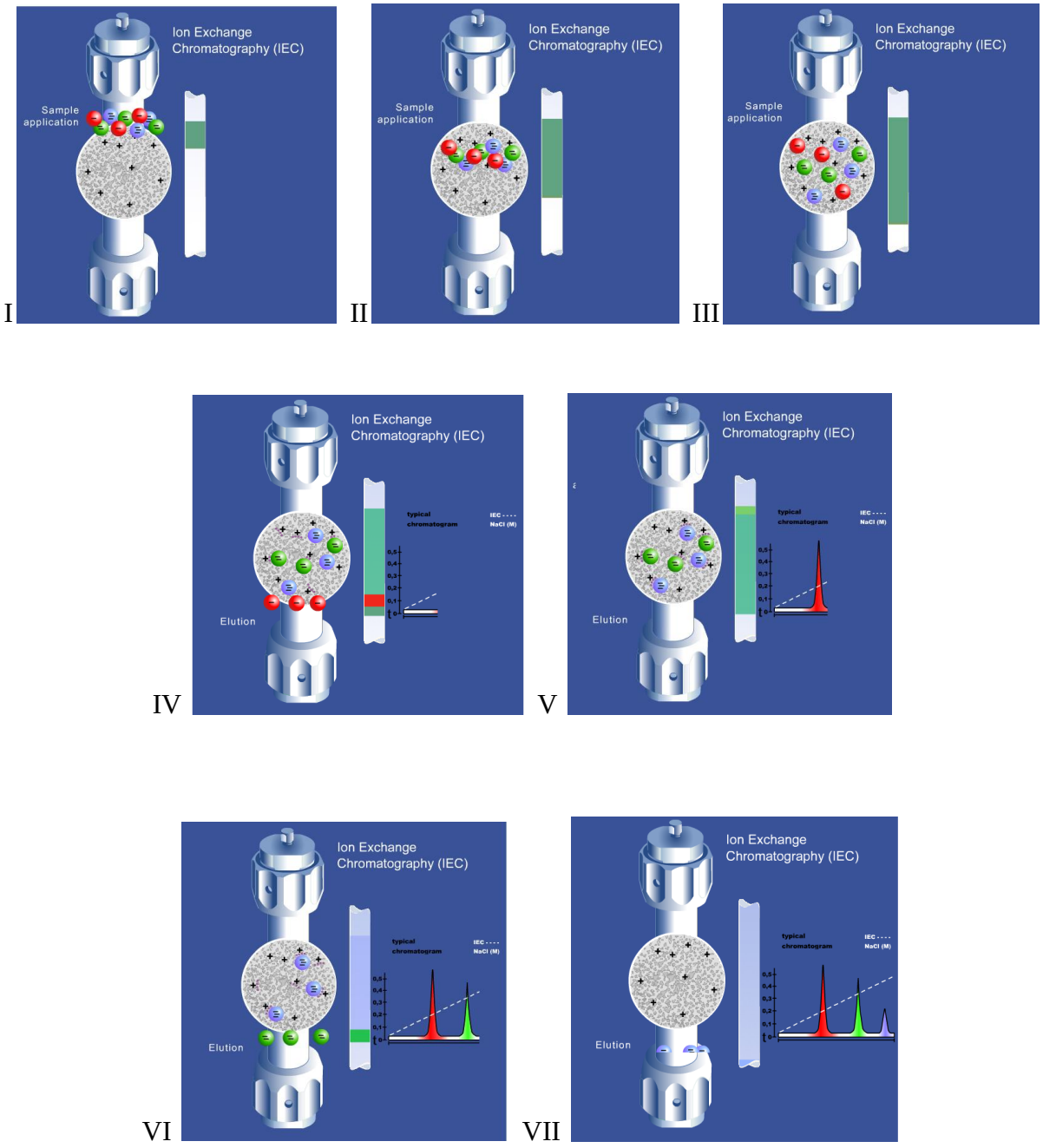

Figure 2-15. Principles of ion-exchange chromatography (36).

2.6.1.2. Buffer pH

The pH of the mobile phase or 'buffer' is taken to be between the pI(isoelectric point) of the protein and the pI of the charged functional group on the stationary phase. In anion exchange chromatography a protein with a pI of 6.8 could run in a mobile phase buffer at pH 8.0 when the pI of the stationary phase is 10.3. Effects of pH have also been discussed in Section 2.5.1.1.

2.6.1.3. Salt and pH Gradients

In ion-exchange chromatography a protein sample is injected onto the column under conditions where it will be strongly retained. A gradient of linearly increasing salt concentration is then applied to elute the sample components from the column. Effect of ionic strength of salts have also been discussed in Section 2.5.1.2.

Another method to elute a column is to use pH to affect a separation. In cation exchange chromatography, raising the pH of the mobile phase buffer will cause the protein to become less protonated and hence less positively charged. The result is that the protein no longer can form a ionic interaction with the negatively charged solid support, which ultimately results in the molecule to elute from the column. In anion exchange chromatography, lowering the pH of the mobile phase buffer will cause the protein to become more protonated and hence more positively (and less negatively) charged. The result is that the protein no longer can form a ionic interaction with the positively charged groups on the surface of the stationary phase which causes the molecule to elute from the column.

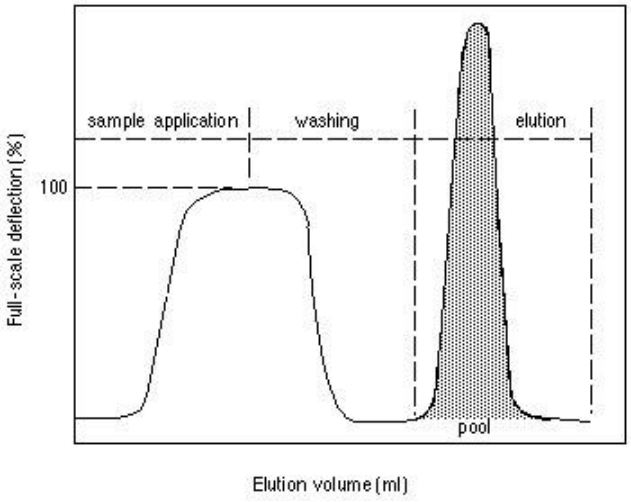

Figure 2-16. A typical protein loading and elution curve displayed by the UV detector of a HPLC or AKTA™ system.

2.6.2. HPLC AND AKTA™ FPLC INSTRUMENTS

High performance liquid chromatography (HPLC) and the Fast protein liquid chromatography (FPLC) are basically a highly improved form of column chromatography. Instead of a solvent being allowed to drip through a column under gravity, it is forced through under high pressures, making it a faster process.

Figure 2.16. illustrates a typical output reading by a UV detector attached to the HPLC or FPLC system, the first peak is formed when the column is exposed to protein 'sample application', the column is then washed till the adsorption falls back to baseline 'washing' the column is then 'eluted' this causes the second peak and samples are collected for concentration analysis 'pool'. The equilibrium protein binding capacity when defined in

terms of the concentration of protein sample/pool collected during elution of a column is ‘mg(protein)/g(fiber)’.

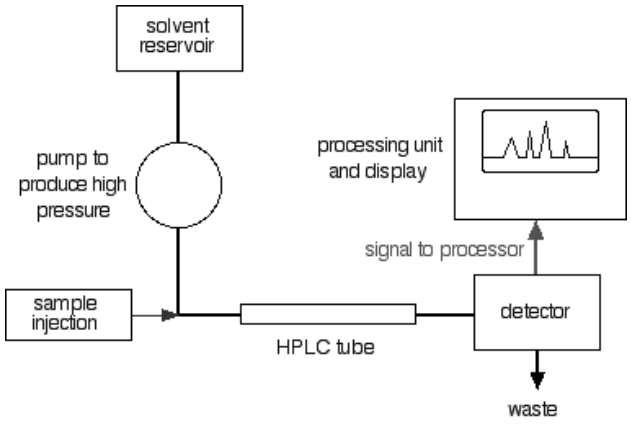

Figure 2-17. Schematic of the HPLC & AKTA systems.

Only difference with FPLC and the HPLC is pressure and flow rate of mobile phase. The HPLC is best for smaller column matrix since it works under increased pressure and it allows solute to equilibrate between mobile and stationary phase faster. Hence, making it a better choice for analytical analysis. However, with the AKTA™ FPLC higher flow rates of the mobile phase can be achieved.

2.6.2.1. Injection of the sample

After the column is equilibrated with the mobile phase buffer overnight, it can then be exposed to a solution of protein that requires separation, this is done by injecting fixed volume into the column. Injection of the sample can be manual or automated.

2.6.2.2. Retention time

The time taken for a particular ‘entity’ (i.e. protein, compound, molecule) to travel through the column to the detector is known as its retention time. This time is measured from the time at which the sample is injected to the point at which the display shows a maximum peak height for that compound. Different compounds have different retention times. For a particular ‘entity’, the retention time will depend on:

- Pressure/flowrate
- Stationary phase
- Solvent
- Temperature of the column

2.6.2.3. The UV detector

Various wavelengths of UV radiation can be adsorbed by organic compounds of different types. If a stream of liquid flowing out of the column is subjected to a beam of UV radiation that is made to pass through it, with a UV detector on the opposite side of the stream, a constant monitoring of how much UV radiation is absorbed by the components present in the stream can be evaluated. The amount of radiation absorbed will depend on the amount of a particular compound that is passing through the beam at the time. Amino acids containing aromatic side chains (i.e., tyrosine, phenylalanine and tryptophan) exhibit strong UV-radiation absorption, proteins and peptides absorb UV in proportion to their aromatic amino acid content and total concentration.

SECTION 3. EXPERIMENTAL

3.1. MATERIALS

In this research, Poly(butylene terephathalate) PBT Celanex© (2003-2) Grade, from Ticona was used to produce melt blown (MB) nonwoven substrates.

Glycidyl methacrylate (GMA) monomer, Diethyl amine (DEA) (CAS No. 109-89-7) was ordered from Fisher Scientific. A pre-packed Sigma inhibitor remover column was used to remove inhibitors from GMA (Product: 306320, St. Louis, MO).

1-Butanol was obtained from Fisher Chemical (Fairlawn, NJ; Grade: ACS), Tetrahydrofuran (THF) and methanol were obtained from Sigma-Aldrich (St. Louis, MO). All solvents were used without purification. Benzophenone (BP) and Phosphate buffer saline (PBS pH 7.4) was ordered from Sigma-Aldrich (St. Louis, MO). Protein Bovine serum albumin (BSA) was ordered from Sigma-Aldrich (Fluka 64161).

3.2. WATER CONTENT ANALYSIS

A moisture analyzer Vapor Pro from Computrac with a detection limit of 10 ppm was used to study the moisture content in the PBT pellets before the resin was introduced to the MB line extruder.

The instrument heated a certain weighted mass of resin test in a septum bottle and the evolved moisture is made to passed through an analysis cell, where the moisture content of the flowing gas is measured. The data is analyzed and converted into micrograms of water for display.

The idea behind measuring the moisture content in the PBT pellets was to be able to control the viscosity of the polymer can be with cracking or hydrolysis of the PBT within the extruder. The aim was that a certain control with viscosity would give us a control on the die block pressure and also the fiber diameter without changing the polymer grade or type. The heating range of the Vapor Pro is 25°C to 275°C. Test parameters such as sample size, heater temperature and test time can be optimized for speed and accuracy.

3.3. POLYBUTYLENE TEREPHATALATE (PBT) MELTBLOWN SUBSTRATES

3.3.1. Meltblown PBT substrate production

The PBT Celanex© resin with 60% and 100% moisture content were melt blown on the Hill's Meltblowing (MB) sample line in the Fiber Science Lab (NWI) at the College of Textiles to produce nonwoven substrate with various fiber diameter distributions. Details of the processing conditions are given in Table 3.1.

Table 3.1 MB processing parameters

MB Line Constants				
Hot Air temperature : 402 °C				
Die to collector distance : 10-15 cm				
Hole diameter :120-130 µm				
Collector: Manually collected				
Extruder Zone Temperature (°C)				
Hot Air	**Zone 1**	**Zone 2**	**Zone 3**	**Air Heater**
402	**280**	**299**	**258**	**550**

Table 3.2 MB processing parameters variables

Variables	1	2	3
Moisture (%)	**100%**	**60%**	
Air Pump pressure*	**20**	**40**	
Throughput (ghm)	**0.08**	**0.20**	**0.26**

***Air velocity is defined in terms of air pump pressure**

3.3.2. Lamination of PBT MB Nonwoven substrate

The PBT MB substrates (A, B, C, D and E) produced from the sample MB line were laminated at 135 ºC @ 10,25,50 psi by Stork MTC 101-1000 layered together to get a similar basis weight of 55±5 gsm.

3.3.3. Basis weight , Thickness, Solidity and Intrinsic surface area studies

Nonwoven substrate basis weight is an important factor that determine their other properties such as strength, porosity. The basis weight of the PBT meltblown substrates was evaluated using 'Standard Test Method for Mass Unit Area of Nonwoven Fabrics' (ASTM D6242-98). All substrates were conditioned at 65±2% relative humidity and 21±1°C temperature prior to testing. Specimens with specific length and width were cut from each substrate type (A, B, C, D and E) and weighed. The mass per unit area was calculated for each PBT MB substrate to the nearest 0.1 g/cm^2 using the following equation:

$$GSM = M/A \quad \text{……(2)}$$

GSM is mass per unit area, (g/ m^2); M is mass of specimen, (g); A is area of specimen (m^2).

The average values of the fabric basis weight and standard deviation for each sample were reported.

The thickness of the substrates was evaluated using AMES (model BG1110-1-04) as the distance between the upper and the lower surfaces of the material, measured under a constant specified pressure.

Solidity of the nonwoven substrate is a dimensionless value that is calculated using the following equation:

Solidity = GSM/ (Polymer δ x **Substrate thickness)…….(3)**

GSM is the substrate basis weight (g/m^2) , polymer δ (g/m^3) is the density of the polymer and substrate thickness (m) is the measured thickness of the substrate. Solidity of the substrate gives an idea of the void space within the material, or the space within the material that is not occupied by polymer.

Intrinsic surface area of the fibers can be calculated as:

AREA/MASS= 4/(Df x δp)……(4)

This is defined as the surface area available for adsorption of protein, Df is the mean fiber diameter (m), δp is the polymer density (g/m^3) (PBT density= $1.31 g/m^3$)

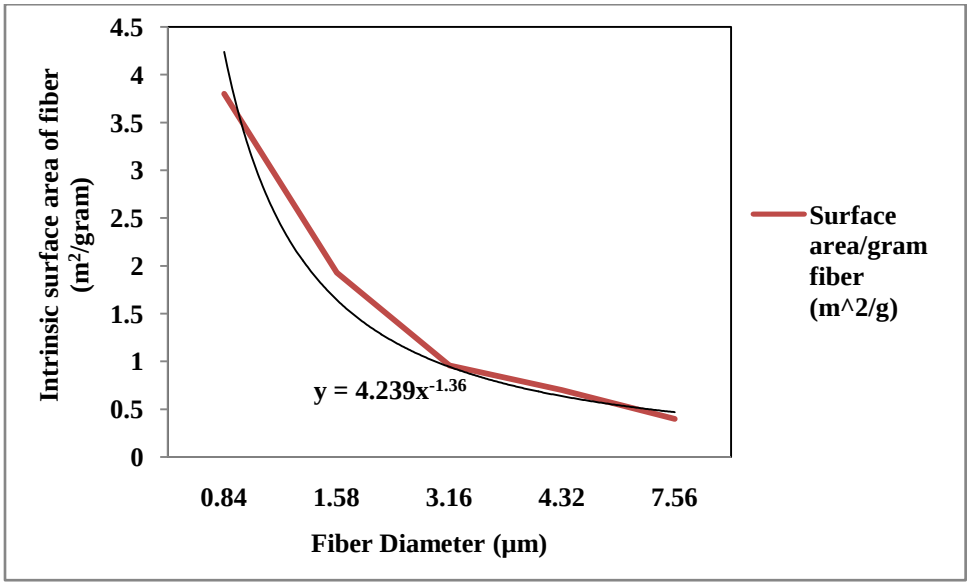

Figure 3-1. Intrinsic surface area vs. fiber diameter.

Table 3.3 Estimated intrinsic surface area of fiber (m^2/g) calculated from fiber diameter

Fiber Diameter (µm)	Area/Mass (m^2/g)
0.84 µm	3.80
1.58 µm	1.93
3.16 µm	0.96
4.32 µm	0.70
7.56 µm	0.40

3.3.4. Pore size distribution analysis

The PMI's Capillary Flow Porometer (model. No. CFP-1100-AX) is an instrument that allows the analysis of nonwoven meltblown substrate . Data was recorded in terms of Bubble Point (largest pore), Mean Pore Size and Pore Size Distribution. PBT melt blown substrates were cut into 5 cm diameter disks and wetted in SILWICK with surface tension of 20.1 dynes/cm and loaded in the instrument, gas was made to pass though the wetted substrate.

Bubble Point (largest pore) The SILWICK wetted sample is stars to become gas permeable at a specific pressure point.

Pore Size Distribution Permeability weighted pore size distribution that is calculated from wet flow curve and dry flow curve indicated for the substrate.

Mean Flow Pore Size A point where the wet flow value is half of the dry flow, a pore size is indicated for the substrate.

The basic principle of pore size measurements is that liquid filled pores of certain surface tension liquid, become gas permeable at a certain pressure, as the liquid is displaced by the gas. This pressure greatly relies on the surface tension of the liquid and the pore size . As nonwoven substrates have a distribution of pore sizes, the pressure at which the first liquid filled pores become gas permeable corresponds to the opening pressure of the biggest pores. By further increasing the pressure drop across the material and measuring the volumetric flow rate, it is possible to obtain data from which the pore size distribution can be calculated.

3.3.5. Tensile studies of PBT Meltblown substrates

The Instron tensile strength tester was used to test the tensile properties of substrates as per ASTM D5034-09 'Standard Test Method for Breaking Strength and Elongation of Textile Fabrics (Grab Test)'. All samples were conditioned to the standard testing conditions 65±2% relative humidity and 21±1°C temperature prior to testing. A gauge length of 3 inch, load cell of 5 lbf and 50kg were used, with a break sensitivity of 50% and a cross head speed of 12 in/min was used for this method. Sample size of 6 samples of dimensions of 1"x6" was used.

3.3.6. FTIR spectroscopy of PBT MB substrate

Attenuated total reflectance (ATR) spectra were collected by FTIR-ATR (Thermo-Nicolet Nexus™ 470-FTIR,Waltham,MA) spectrometer, with a germanium crystal , equipped with an Advantage microscope and using liquid nitrogen cooled Mercury Cadmium Telluride (MCT) detector. At least 64 scans were obtained to achieve an adequate signal to noise ratio. The spectral resolution was 4 cm^{-1} . The depth of penetration of the FTIR was 0.67µm.

3.3.7. Scanning electron microscopy (SEM) of PBT MB substrate fiber diameter distribution and study of substrate surface post lamination

Fiber morphology of the PBT nonwoven substrate was observed with an Hitachi S-3200N Scanning Electron Microscope (SEM). The samples were fixed onto a sample holder using carbon tape and splutter coated with Pd/Au alloy in the presence of Argon gas.

To characterize fiber diameter distribution of the various nonwoven substrates, non laminated samples were considered and diameters of more than 100 fibers were measured for each.

In the case of laminated substrates , the surface of the substrates were observed for fiber deformation.

3.4. GLYCIDAL METHACRYLATE (GMA) AND DIMETHYLAMINE (DEA) TREATMENT OF POLYBUTYLENE TEREPHATALETE (PBT) MELTBLOWN SUBSTRATE

3.4.1. GMA-DEA treatment of PBT MB substrate

PBT nonwoven substrates of controlled basis weight of aprox. ~55gsm and five different mean fiber diameters, were cut in size of 5x7.5 cm^2 , these were weighed and were subjected to UV-initialized grafting of GMA at 365 nm in the presence of benzophenone (BP).

The grafting step was carried out with a UV lamp (EA-180,Spectroline, Westbury, NY)of intensity 5mW/cm^2. Each sample was sprayed with 1.5ml 20%(v/v) GMA in butanol solution containing 1.3% (w/w) benzophenone (initiator to monomer ratio=1:25).

The sample was then sandwiched between two glass slides and put under the UV lamp for grafting. After grafting unreacted monomer, homopolymer and benzophenone were removed from the sample by sonication in THF and methanol, each for 30min.

The sample was then dried in air and analyzed by FTIR and SEM. The samples were then submerged in a 20%(v/v) Diethyl amine (DEA) in water solution. These were left submerged in erlenmeyer flasks at 25°C shaker bath for 5.2 hours.

The samples were then removed and washed in DI water thoroughly before they were left to dry under standard conditions of 65±2% relative humidity and 21±1°C temperature.

3.4.2. Weight gain analysis after GMA-DEA treatment of PBT MB substrate

The Weight Gain (WG%) was determined by calculating the percentage increase in weight as described, where W' and W'' represent the weights of the initial and grafted polymer respectively. The samples were weighted in an analytical balance.

Weight gain (WG %) = (W"-W')/W' x 100…….(5)

The samples were studied for a change in weight after grafting of PBT nonwoven substrates by weight measurement on an electronic digital balance. For higher accuracy, the samples were weighed in grams rounded off to the 4th decimal place.

3.4.3. Tensile studies and FTIR of PBT MB substrate post GMA-DEA treatment

Tensile and FTIR studies for nonwovens post grafting were done similar to those for the untreated PBT nonwoven substrate.

3.4.4. SEM of PBT MB substrate post GMA-DEA treatment

Fiber morphology of the PBT nonwoven substrate was observed with an Hitachi S-3200N Scanning Electron Microscope (SEM). The samples were fixed onto a sample holder using carbon tape and splutter coated with Pd/Au alloy in the presence of Argon gas.

3.5. HIGH PROTEIN LIQUID CHROMATOGRAPHY (HPLC) AND AKTA™ FPLC PURIFIER

3.5.1. Exposure of Bovine Serum Albumin (BSA) protein to packed column (HPLC)

GMA-DEA treated PBT MB substrates were cut into discs (sample size 30) and packed into

a 1.1cm diameter adjustable volume Vantage-L column (Millipore™, Billerica, MA). The column was mounted to a Waters 616 LC system (Waters Corporation™, Milford, MA) and equilibrated by passing the PBS pH 7.4 buffer overnight. Injections of 1.5ml BSA solution of 10 mg/ml concentration were made at flowrates 0.5 ml/min and 0.08ml/min.

When the binding capacity of the column was reached, the column was washed with PBS until the effluent concentration fell back to a baseline value. The effluent concentration of BSA was measured with UV absorbance at 280nm by a Waters 2487 UV detector (Waters Corporation™, Milford, MA). Bound BSA was eluted with 1M NaCl in PBS pH 7.4. The dead volume of the system was determined by acetone injections.

3.5.2. Exposure of Bovine Serum Albumin (BSA) protein to packed column (AKTA™)

GMA-DEA treated PBT MB substrates were cut into discs (sample size 90) and packed into a 1.1cm diameter adjustable volume Vantage-L column (Millipore™, Billerica, MA).
The column was mounted to a GE AKTA™ FPLC system (GE Healthcare™, Pittsburgh PA) and equilibrated by passing the PBS pH 7.4 buffer overnight. Injections of 10 ml BSA solution of 10 mg/ml concentration were made at flowrates 1 ml/min and 4 ml/min. When the binding capacity of the column was reached, the column was washed with PBS until the effluent concentration fell back to a baseline value. The effluent concentration of BSA was measured with UV absorbance at 280nm by a GE 2487 UV detector (GE Healthcare™ Pittsburgh, PA). Bound BSA was eluted with 1M NaCl in PBS pH 7.4.

3.5.3. Sample collection and BCA protein concentration evaluation

Proteins and peptides absorb UV-light in proportion to their aromatic amino acid content and total concentration, this can be detected using a UV spectrophotometer. For a given protein where the amino acid composition has been defined, it can be observed that, an absorptive coefficient can be obtained; further, the protein's concentration can be calculated using the adsorptive coefficient. For proteins of concentrations as low as 100 μg/ml, can be detected using UV detector. However, for aqueous protein solutions measuring absorbances are usually done at UV wavelengths of 280 nm.

Describing a UV spectrophotometer, monochromatic plane-parallel radiation enters a sample (containing protein) at right angles to the plane-surface. It can then be stated that the transmittance and absorbance of a sample(containing protein) depends on the molar concentration(c), light path length in centimeters (L), and molar absorptivity (ε) for the dissolved substance.

$$\mathbf{T = 10\varepsilon cL \text{ or } A\lambda = \varepsilon\, c\, L \ldots\ldots\ldots\ldots\ldots\ldots (6)}$$

Through Beer's Law, 'molar absorptivity' is a constant and the absorbance is proportional to protein concentration measured at a given wavelength. Since, laboratory UV spectrophotometers are fitted for use with 1 cm width sample cuvettes; hence, the path length is concered to be equal to one.

$$A\lambda = \varepsilon\, c\, L = \varepsilon\, c \text{ when } L = 1 \text{ cm} \ldots\ldots\ldots\ldots\ldots..(7)$$

3.5.3.1. UV-VIS Spectrophotometer was used to evaluate protein concentration

BSA effluent concentrations that were collected during elution of the columns were measured using a Shimadzu 160UV Spectrophotometer.

3.5.3.2. BCA™ protein assay kit

The BSA concentration of the effluent was measured by the bicinchoninic acid (BCA) method BCA™ protein assay kit. This kit analyzes the know protein concentration (calibration curve) and plots the unknown effluent concentration (collected sample) value against it. The data is collected as a result of the comparison between the known and unknown concentrations.

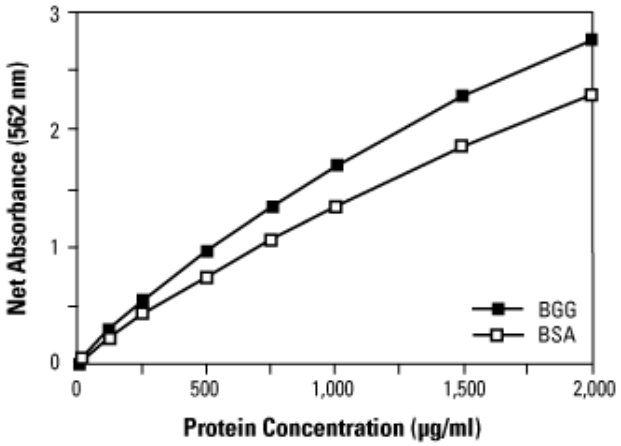

Figure 3-2. BCA™ calibration curve.

SECTION 4. RESULTS AND DISCUSSION

The results and discussions will be discussed in three parts, first in terms of, characterization of PBT MB substrate process-structure-property relationship, characterization of PBT substrate post grafting with GMA-DEA and analysis of protein adsorption by PBT MB treated substrates.

4.1. PBT Meltblown substrate : Process-Structure-Property Relationship

4.1.1. PBT Meltblown substrate formation

As previously highlighted, a relationship between intrinsic surface area of fiber and amount of adsorbed protein has been discussed in Section 3.3.3. To start working in this direction it was imperative to develop nonwoven substrates with varying fiber diameter distributions which would provide the required surface area.

The variables used during the production of the PBT MB webs are listed in Table 4.1, here all substrates have been extruded at 0.14ghm. The PBT Celanex© 2003-2 grade is a fiber grade resin which is not completely suitable for meltblowing purposes. We employed hydrolysis or 'cracking' to control viscosity of melt polymer in the extruder, by increasing the moisture content in the resin it was gradually observed that the die block pressure of the sample MB line reduced, however when the moisture content was further increased from 60% to 100% little change was observed in the die block pressure (psi) or in the mean fiber diameter (μm) of the MB substrates, as noted in Figure 4.1.

For a constant melt throughput of 0.14 ghm it was possible to produce mean fiber diameters in the range of 1.58µm to 2.93µm, as noted in Table 4.1. As the moisture content of the resin in the extruder rose the melt viscosity fell causing the die block pressure to fall and the fiber diameter to reduce, as a result, the tensile strength of the fibers would reduce since the molecular wt. of the polymer dropped with hydrolysis (Section 2.1).

Table 4.1 Effect of die block pressure (psi) vs. mean fiber diameter (µm) for PBT MB.

PBT MB substrate ID	100% water content 40psi Air	60% water content 40psi Air	60% water content 20psi Air
***Mean Fiber Dia.**	1.58	1.65	2.93
Std. Dev.	0.30	0.43	0.90
Die Block Pressure	175	185	185

Sample size: * >50

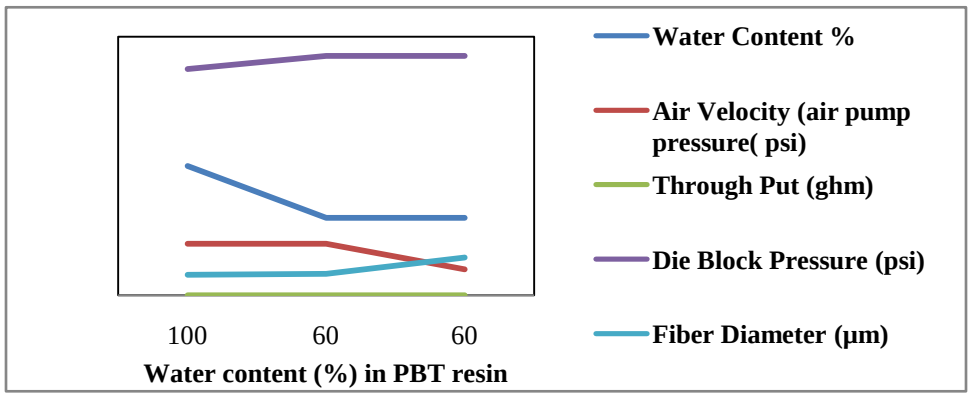

Figure 4-1. Trend for PBT resin with 60% and 100% water content.

To obtain a greater range of mean diameters, melt throughput of 0.08, 0.2 and 0.26 grams per hole per minutes (ghm) were explored (Table 4.2). Melt throughput (ghm) decides the rate and volume of polymer that is pushed out of the die, this in turn influences the fiber diameter distribution. Air pump pressures of 20psi and 40psi were explored for each throughput value. The higher the air pump pressure (psi) that greater the air velocity. In Figure 4.1 it can be observed that for a constant throughput where air velocity changes, a change in mean fiber diameter is observed. Air velocity obtained by pump pressure of above 40 psi value were not used since the webs were manually collected and it was difficult to hold the collector under the die block.

Table 4.2 PBT MB processing parameters for substrates with throughput(ghm) ranging from 0.08 to 0.26

Sample ID for PBT MB	**60% wet-0.08 ghm**	**60% wet-0.20 ghm**	**60% wet-0.20 ghm**	**60% wet-0.26 ghm**	**60% wet-0.26 ghm**
% Wet PBT	60%	60%	60%	60%	60%
Water content (gH2O/Kg PBT)	0.74	0.74	0.74	0.74	0.74
Air Pump Pressure (psi)*	40	40	20	40	20
Throughput (ghm)	0.08	0.20	0.20	0.26	0.26
Die Block Pressure (psi)	65	250	250	350	350

***Air velocity is defined in terms of air pump pressure**

The apparent viscosity of the polymer melt during processing can be controlled through hydrolysis or 'cracking'. The significance of viscosity in melt processing of polymers is that it gives an indication of degradation reactions which lead to a change in molecular weight which is strongly correlated with die block pressure (psi).

4.1.1.1. Fiber Diameter distribution and Mean fiber diameter evaluation of PBT MB nonwoven substrate

Due to the nature of the meltblowing process, fibers produced may or may not have same diameters or shape. This can be observed in Figure 4.2 SEM micrographs of the different substrates, that a range of fiber diameters and fiber shapes can seen in the same web.

Five webs were produced namely substrate A, B, C, D and E. The difference between each of the five substrates are defined by meltblown production variables:

- Polymer throughtput
- Air velocity

Table 4.3 Water content(%), throughput (ghm)and air pump pressure (psi) for PBT MB susbtrate A, B, C, D and E

A	B	C	D	E
60% wet 0.08 ghm (40 PSI Air)	**60% wet 0.20 ghm (40 PSI Air)**	**60% wet 0.26 ghm (40 PSI Air)**	**60% wet 0.20 ghm (20 PSI Air)**	**60% wet 0.26 ghm (20 PSI Air)**

It can also be noted through Figure 4.2, in the SEM micrographs C, D and E (same scale) that density of fibers vary. The fiber diameter seem to increase from substrate A to E, in SEM micrograph of substrate E, the fiber diameter distribution seems very large.

A.

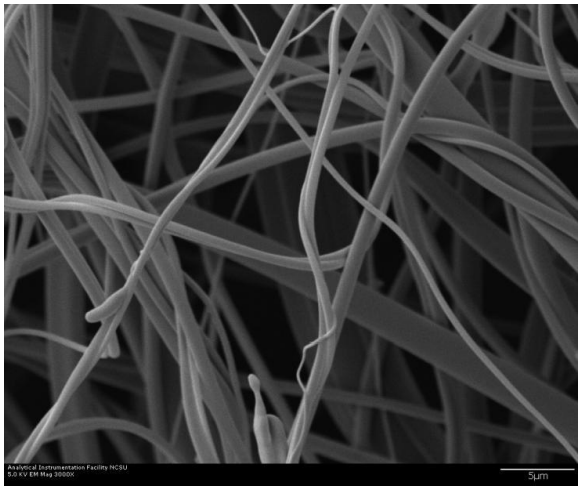

B.

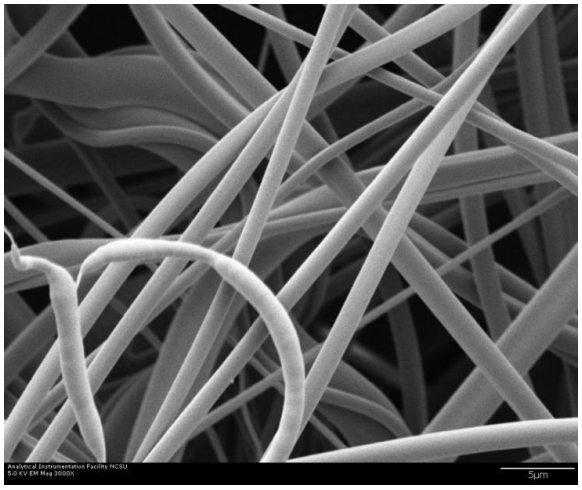

Figure 4-2. SEM micrographs of PBT MB substrates A and B where a range of fiber diameters can be seen.

C.

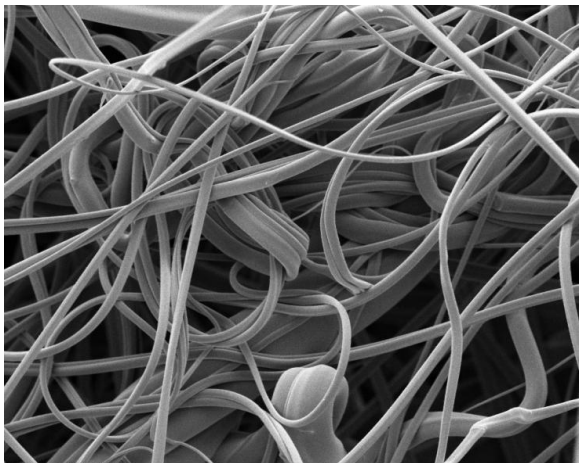

D.

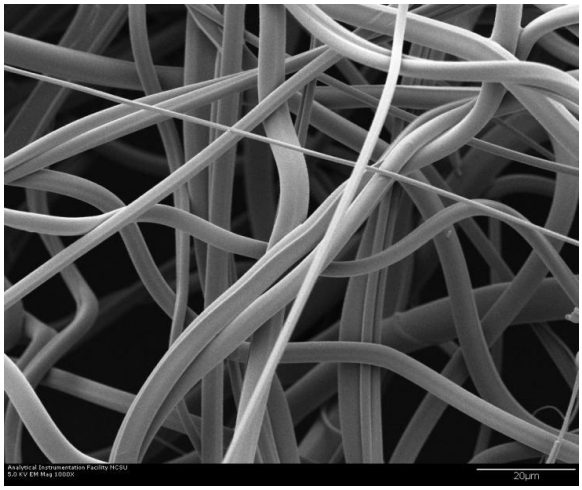

E.

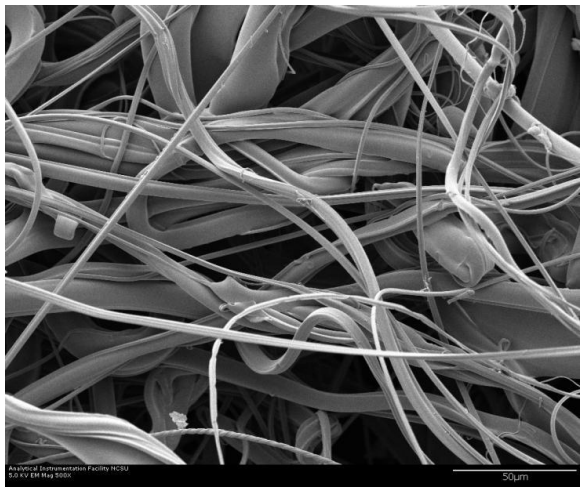

Figure 4-2. SEM micrographs of PBT MB substrates C, D and E where a range of fiber diameters can be seen.

Through SEM micrographs in Figure 4.2, it is apparent that fibers formed during meltblowing have various shapes and are irregular. In the fiber diameter distribution of substrates A, B, C and E as indicated in Figure 4.3 it can be seen, that during production of MB substrates, high air velocity and low melt throughput can lead to smaller diameter fibers as in the case of substrate A, while higher melt throughput and lower air velocity produce larger diameter fibers, as with substrate E. It is also observed in Figure 4.3, that the distribution gradually becomes broader as the fiber diameter increases, in the case of substrate A , the distribution is relatively compact when compared to the distribution of substrate E, this is visually obvious in corresponding SEM micrographs of the two substrates.

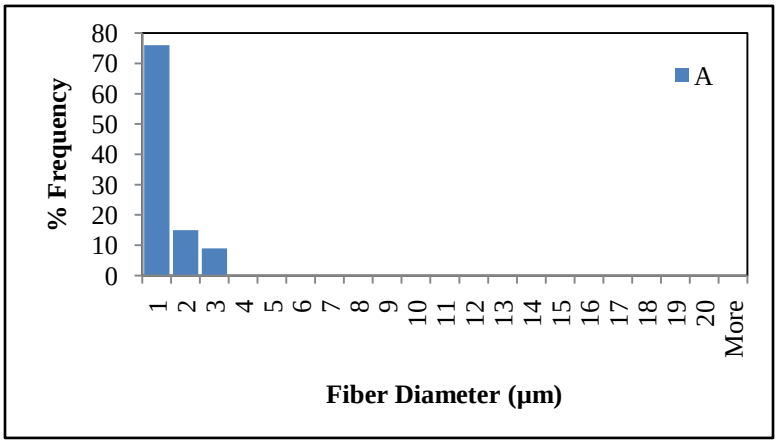

Figure 4-3. Fiber diameter distribution of PBT MB substrates A.

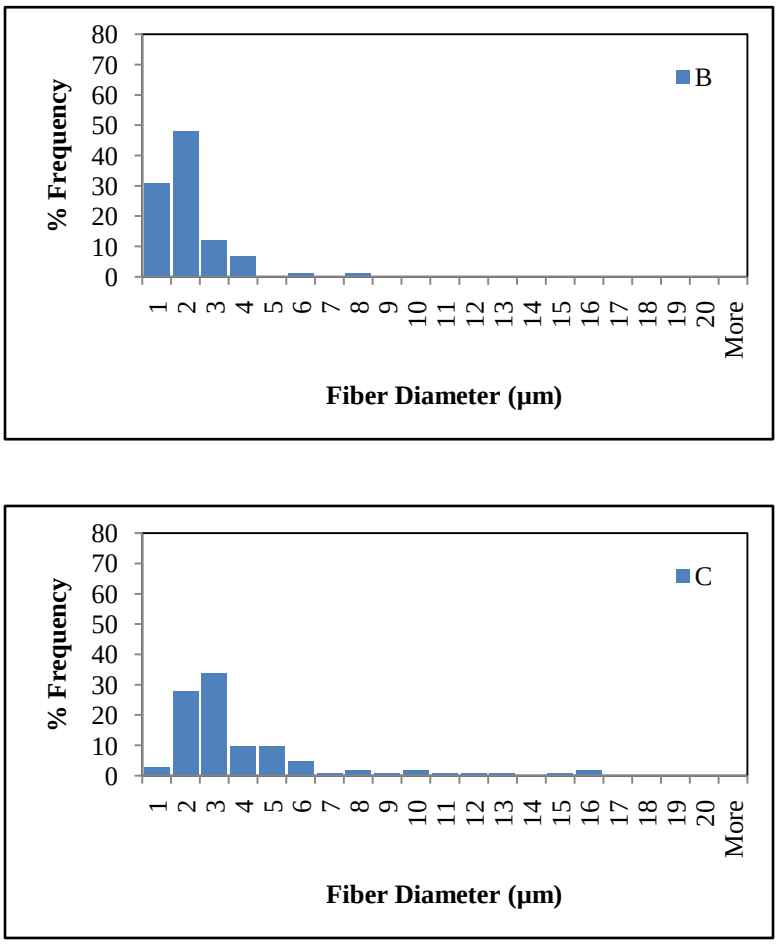

Figure 4-3. Fiber diameter distribution of PBT MB substrates B and C.

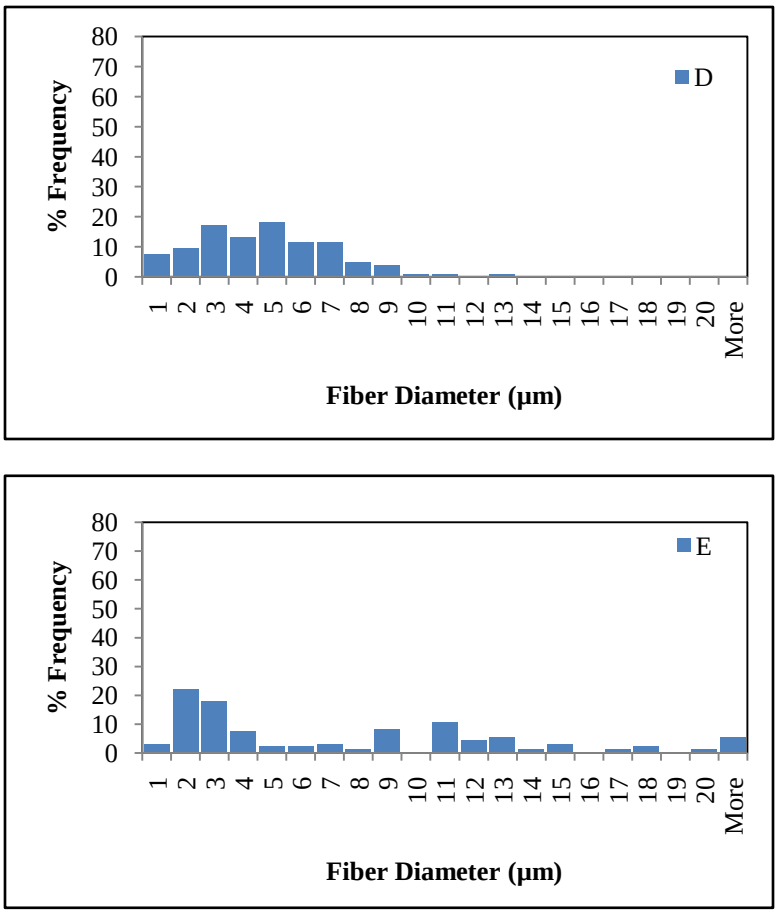

Figure 4-3. Fiber diameter distribution of PBT MB substrates D and E.

In Figure 4.4 and Figure 4.5 it is obvious that the mean fiber diameter increase from substrate A to substrate E, the standard deviation for substrate E is large as noted in the fiber diameter distribution of substrate E. For substrate A, a large number of fibers lie in the bin (0-1) suggesting the presence of nanofibers in the range of 300-1000 nm. For substrate C and E there are few fibers in bin (0-1).

As the throughput increases, there is an increase in the corresponding mean fiber diameter (μm), however, with the decrease in air pump pressure (psi) from 20-40 a corresponding decrease in mean fiber diameter was obtained. It can be noted that the mean fiber diameter of substrate C and substrate D are very similar.

A relationship can be formed between intrinsic surface area and the substrate fiber diameter. For a substrate with smaller mean fiber diameter, intrinsic surface area should be higher as suggested in Figure 4.6. We have attempted to exploit this relationship between fiber diameter and intrinsic surface area during the length of the research, since the surface area provided by smaller fibers is greater, allowing a larger area for grafting of GMA-DEA polymer brushes, this in turn would translate into greater surface available for protein adsorption.

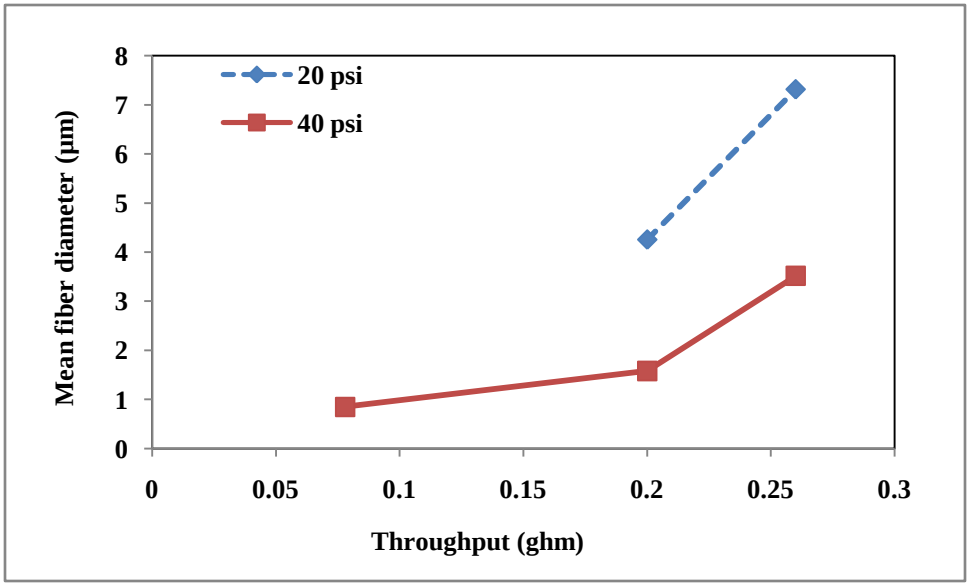

Figure 4-4. PBT MB substrates A,B,C,D and E mean fiber diameters (µm) vs. through-put (ghm) at air pump pressures of 20psi and 40psi.

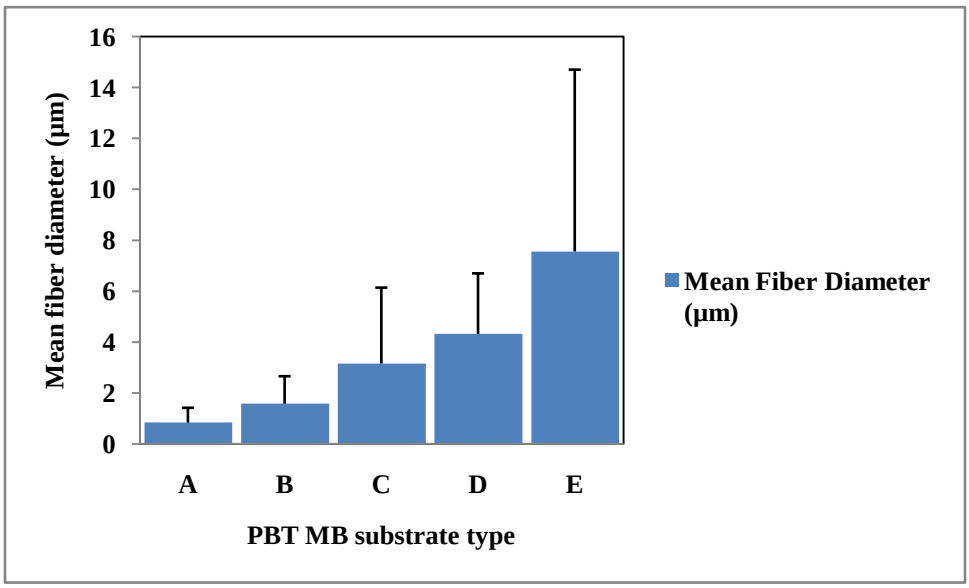

Figure 4-5. Mean fiber diameters of PBT MB substrate A,B,C,D and E.

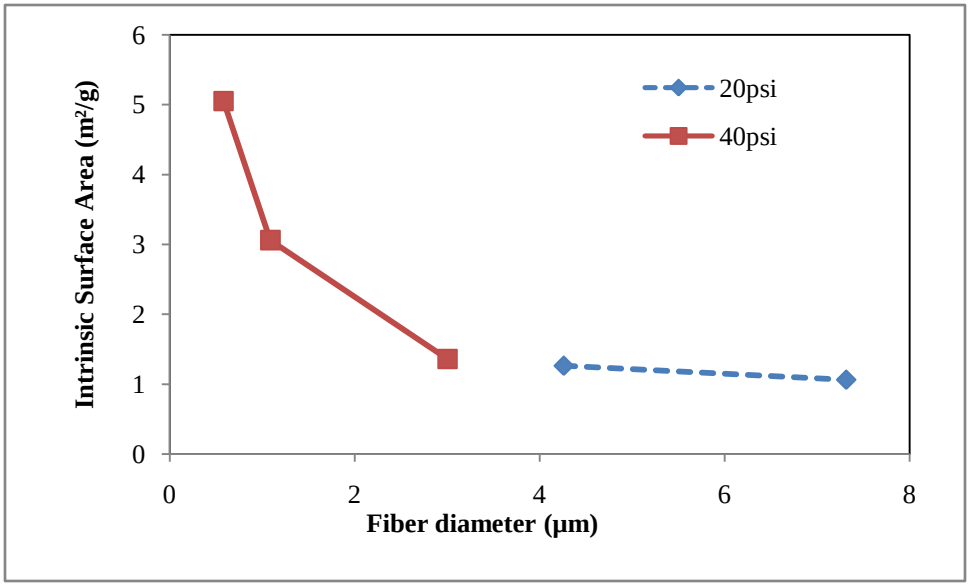

Figure 4-6. Calculated intrinsic surface area (m^2/g) from fiber diameter distribution.

4.1.2. Lamination of PBT MB Nonwoven substrate

The PBT MB nonwoven substrates produced form the sample MB line were layered and weighed to get a similar basis weight of 55±5 gsm. These layered samples were then laminated together. Lamination of the samples influenced its resultant solidity, substrate strength and pore size. One sample substrate from each trial was considered for lamination. Lamination conditions are mentioned in Table 4.4.

Table 4.4 Lamination conditions of PBT MB substrates

Sample ID for PBT MB	**60%wet 0.08ghm (40psi Air)**			**100%wet 0.14ghm (40 psi Air)**			**60% wet 0.14ghm (20psi Air)**		
Lamination at Temperature 135°C	10psi	25psi	50psi	10psi	25psi	50psi	10psi	25psi	50psi

A.

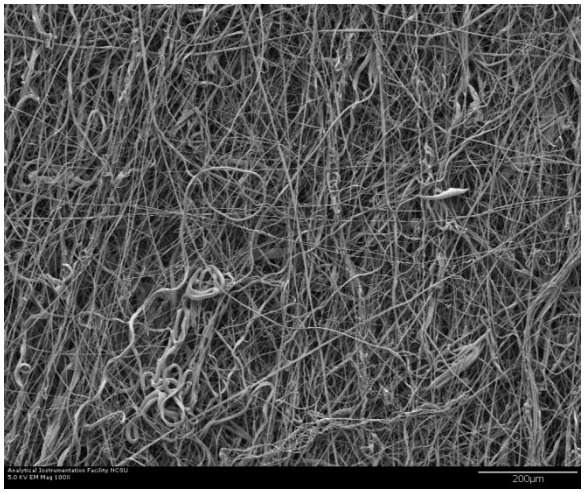

B.

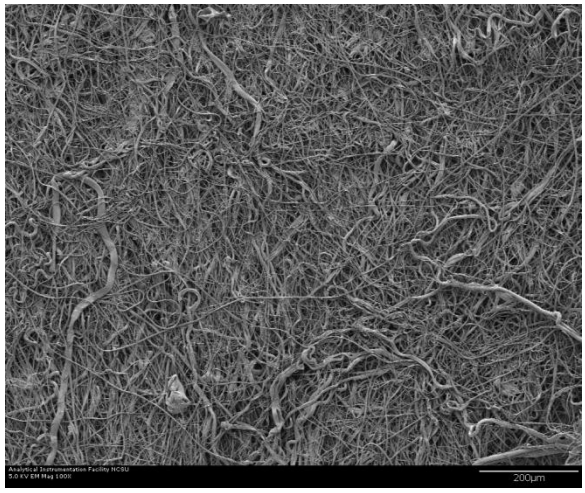

C .

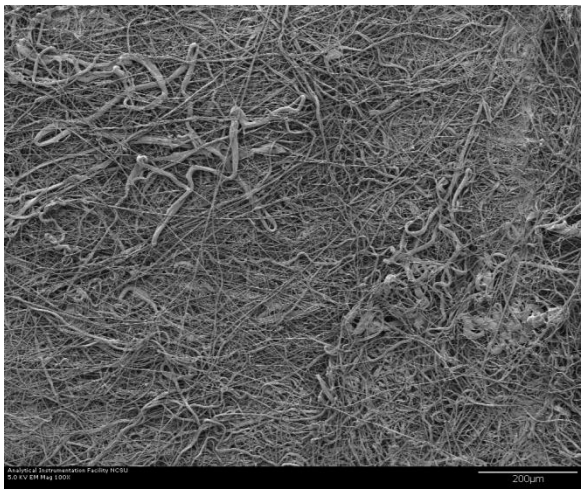

Figure 4-7. SEM micrographs of 60% wet 0.08 ghm PBT MB laminated substrate A.10 PSI, B. 25PSI, C. 50PSI.

A.

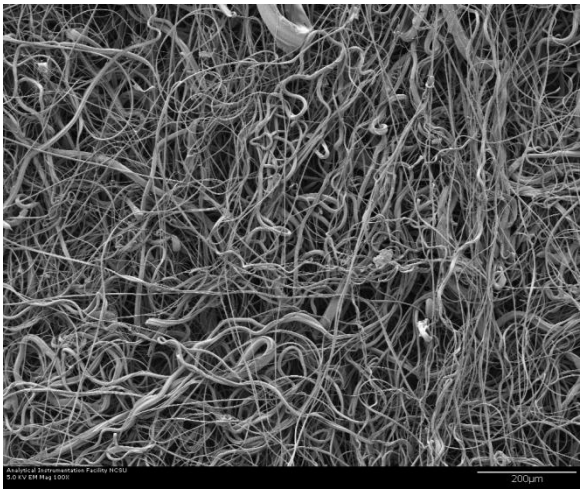

B.

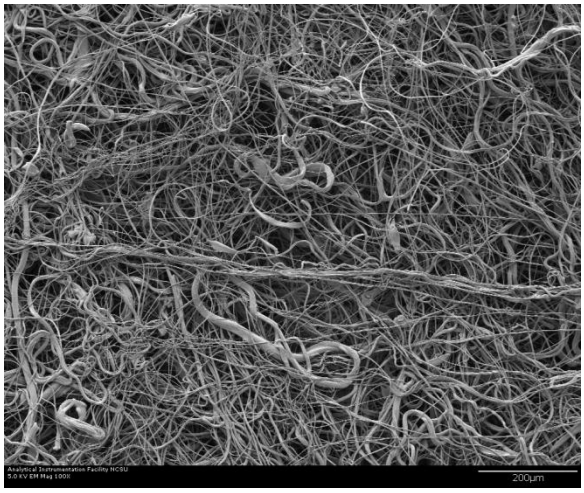

C.

Figure 4-8. SEM micrographs of 60% wet 0.14 ghm PBT MB laminated substrate A. 10 PSI, B. 25PSI, C. 50PSI.

The laminated webs were further evaluated through PMI Capillary Flow Porometer for pore size and SEM for observed surface deformation of fibers. There was a compromise between lamination pressure and resultant poresize. It was observed through SEM micrographs in Figure 4.7 and Figure 4.8 that at 50psi laminator pressure the fibers on the web surface seemed deformed and the corresponding mean pore size increases, as noted in Figure 4.9. However at 10psi nearly no bonding was observed between fibers in the web.

Table 4.5. Lamination condition of PBT MB substrates with resultant poresize (µm) and substrate solidity

Sample ID for PBT MB		**60% wet 0.08 ghm (40 PSI Air)**			**100% wet 0.14 ghm (40 PSI Air)**			**60% wet 0.14 ghm (20 PSI Air)**		
Fiber diameter*	**Mean (µm)**	0.84			1.58			1.63		
	Std. Dev.	0.58			0.30			0.45		
	10 %tile	0.35			1.13			1.78		
	90 %tile	1.47			3.67			3.46		
Lamination Pressure (psi) 135°C		10	25	50	10	25	50	10	25	50
Pore size (µm)**	**Mean**	15.23	3.86	4.70	10.26	7.96	7.53	9.26	7.78	11.16
	Smallest	6.83	1.8	1.76	5.13	4.7	4.13	5.63	4.06	3.06
	Largest	18.26	7.73	7.76	23.96	17.76	15.76	19.96	15.97	16.1
Basis weight (gsm)***		55±3			55± 3			55± 3		
Thickness (mm)******		0.22 ± 0.02			0.26 ± 0.02			0.24 ± 0.04		
Solidity		0.17			0.16			0.17		

Sample size:*>50, **3, ***Std.Dev. of 10samples, ****Std. Dev. of 15 samples.

At 25psi laminator pressure the pore size seems the least, as noted in Figure 4.9, this was then regarded best lamination pressure at 135ºC.The solidity, thickness and basis weight

(gsm) remain nearly constant and this is observed in almost all samples during the length of the research.

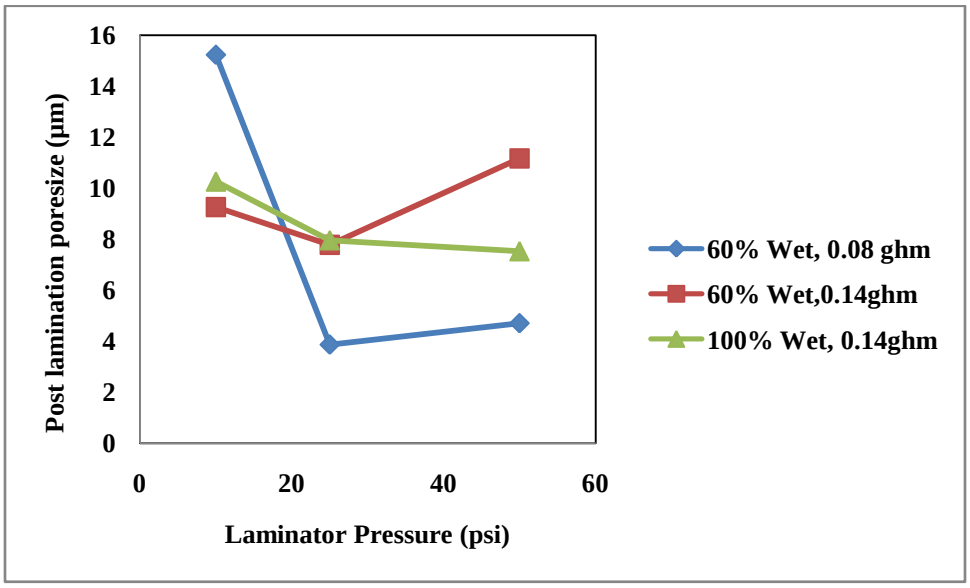

Figure 4-9. PBT MB substrate laminator pressure (psi) vs. mean poresize (µm).

For three PBT MB substrates with mean fiber diameter 0.84µm, 1.58µm, 1.63µm were laminated, it was noted that 25psi @ 135°C show the best lamination condition based on resultant pore size and surface deformation of fibers as seen in micrographs. These conditions were used to laminate samples obtained during final trial. It was also observed that calendering webs between flat calendar roles resulted in film formation of MB samples at least pressure condition (100psi) at 50°C

4.1.3. Basis weight , Thickness and Solidity of PBT MB substrate post lamination

Post lamination substrate properties such as thickness, solidity, basis weight were evaluated and these have been reported in Table 4.6. Though Figure 4.10 it can be noted that while the fiber diameter increases the basis weight , thickness and solidity are almost constant for all five substrates.

Table 4.6. PBT MB substrate A, B, C, D and E post lamination

PBT MB Subtrate ID	A	B	C	D	E
Thickness (mm)*	0.33	0.35	0.36	0.43	0.36
Solidity	0.12	0.11	0.11	0.09	0.11
Basis Weight (gsm)**	55±1	55±3	55±4	55±4	55±10
Mean fiber dia. (µm)***	0.84	1.58	3.16	4.32	7.56

Sample size: *15, **Std. Dev. of 10 samples, *>50**

Basis weight (gsm) is the mass of polymer per meter of the substrate, as noted in Table 4.6. Basis weight (37) is an important factor while considering developing a filter for protein adsorption, however since A, B, C, D and E , PBT MB substrates have been produced on a sampling MB line we have considered a mean basis weight of ~55 gsm. The basis weights for all substrates are almost constant, however for substrate E there is a higher deviation from mean.

Solidity is a dimensional less unit, it defines the mass of polymer per unit volume of the substrate. This substrate property is different from void volume or porosity since, substrate

solidity can be very similar, however, for a certain mass of polymer per unit volume ,the number of fiber in that unit area would give the indication of the compactness of the structure or void spaces within the structure.

With lamination conditions for all five substrates A, B, C, D and E being the same, the thickness and the basis weight being similar, the resultant solidity is similar, we expect mean pore size to increase with the increase in fiber diameter since the porosity or void spaces within substrate would increase per unit volume, suggesting fibers with larger diameters.

The substrate thickness playes and important role during the grafting process. Before exposing the substrate to UV, it is wetted in a monomer-initiator solution. The amount of solution held within the pores is defined by:

- Amount/structure void space present within the substrate
- Influence of fiber diameter
- Effect surface tension between fiber and liquid

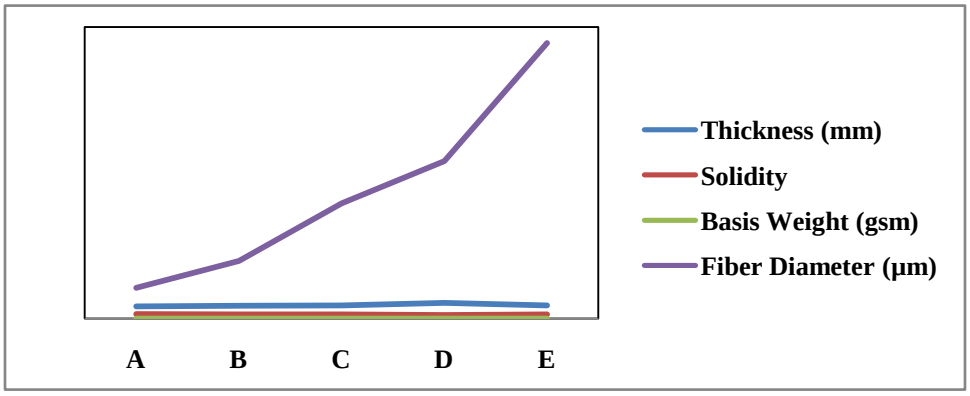

Figure 4-10. PBT MB trend for thickness, solidity, basis weight and mean fiber diameter post lamination of A, B, C, D and E.

It was noted that while the mean fiber diameter for the five PBT MB substrates increase, the thickness , solidity , basis weight nearly remain constant post lamination. A slight increase in thickness is observed for substrate D. The post lamination properties of substrates provided a platform on which further evaluation of substrates A, B, C, D and E took place.

4.1.4. Poresize evaluation of PBT MB substrates post lamination

There is a general trend (Figure 4.11) suggesting increase in poresize for substrates A to substrate E. It can be noted in Figure 4.12 that with the increase in melt throughput during web formation the pore size of the PBT MB substrate increases. During the meltblowing process as fibers are randomly being laid and bonded at the same time, the factor

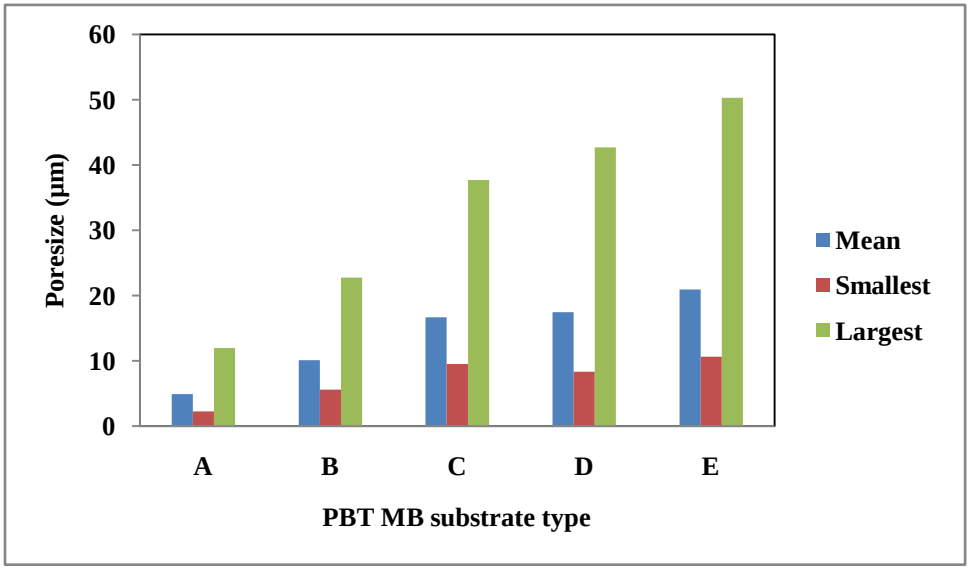

Figure 4-11. Poresize distribution for PBT MB substrate A, B, C, D and E.

that influences the bulk volume is primarily the fiber diameter. As shown in Figure 4.13 with the increase in fiber diameter there is an increase in the mean pore size.

During formation of substrates A, B and C fibers were attenuated using the air velocity i.e.40 psi pump pressure, however the melt throughput increased from 0.08 ghm to 0.26ghm. In the case of substrate D and E, fibers were attenuated using air velocity i.e. 20 psi pump pressure while melt throughput of 0.20ghm and 0.26ghm was used respectively.

Due to this reason there is a change in trend observed along the length of the curves as indicated in Figure 4.13, however the overall trend suggests that increase in fiber diameter and poresize go hand in hand. The posesize for substrate C and D are not greatly different hence, as the fiber diameter increases from ~3µm to ~4µm the poresize is nearly constant.

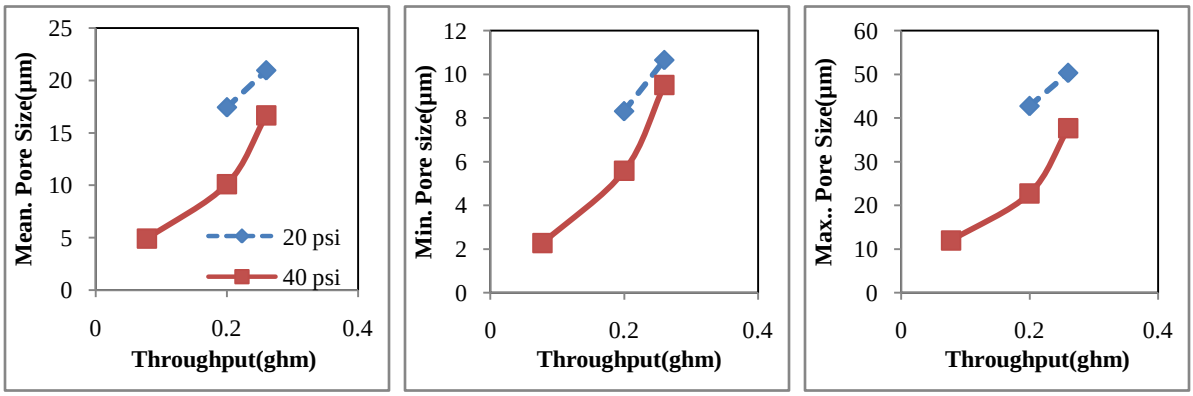

Figure 4-12. PBT MB substrate A,B,C,D and E mean, maximum and minimum poresize (µm) vs. throughput (ghm).

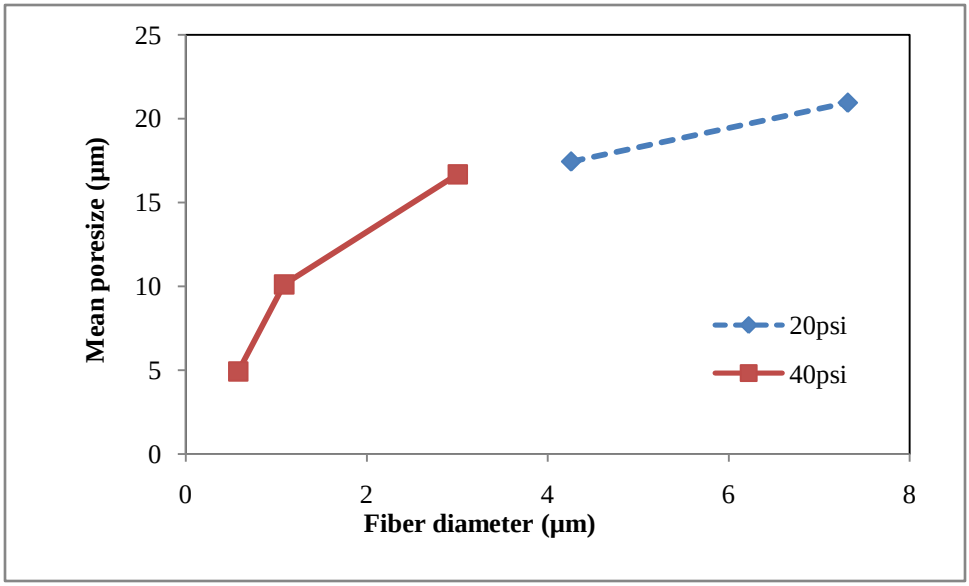

Figure 4-13. PBT MB substrate A, B, C, D and E mean poresize (µm) vs. mean fiber diameter (µm).

4.1.5. Tensile strength evaluation of PBT MB nonwoven substrate in the MD

Due to the size of the die block of the MB line it was not possible to produce web beyond a certain width, however, any length of web along the machine direction was possible. In Figure 4.14 it can be observed that with increase in fiber diameter there is a gradual decrease in peak load (lbf), however for substrate A the peak load is lower than for substrate B.

In Figure 4.17 and Figure 4.16 it can be observed that substrate A and B show an increase peak load(lbf) however the strain at break(%) for A and B is low , indicating higher modulus this can be attributed to better web entanglement due to finer fibers.

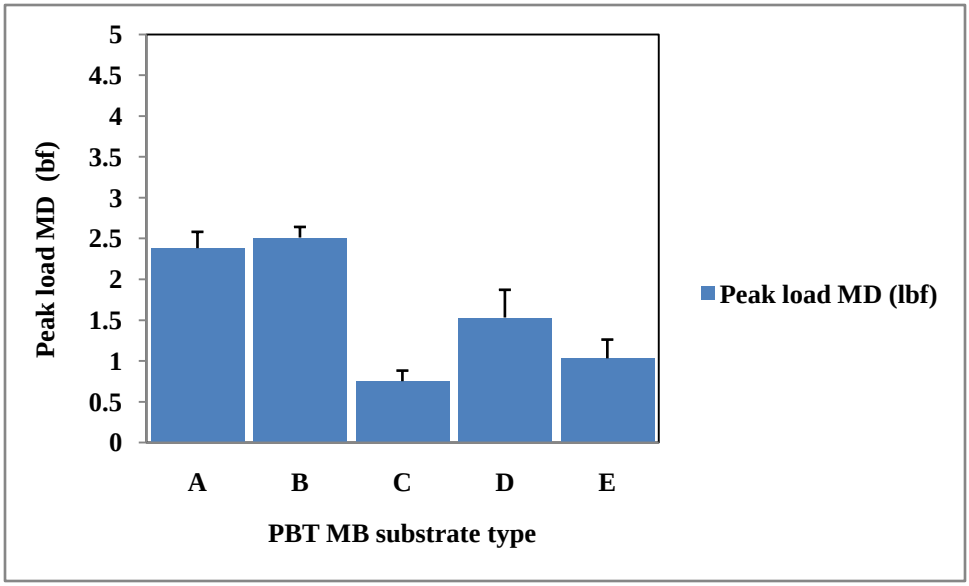

Figure 4-14. Peak loads demonstrated by PBT MB substrates A, B, C, D and E.

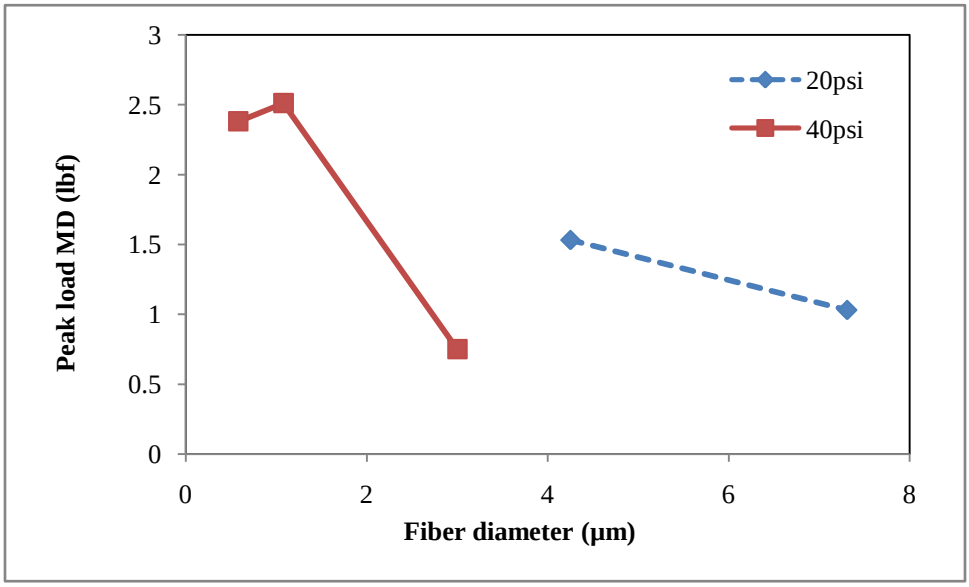

Figure 4-15. Peak load (lbf) vs. meanfiber diameter (µm) of PBT MB substrates.

In the case of substrate A and B due to smaller fibers present in the web it is possible that increased friction between fibers keep the integrity of the web intact while under stress resisting strain.

To support this idea, in Figure 4.16, it can be observed that, peak load decreases as meanpore size and fiber diameter increases, particularly in the case of substrate C. Further in comparison between substrate C and D the mean pore size seems nearly constant, the peak load increases in the case of substrate D since the mean fiber diameter is greater for substrate D, while for substrate E the poresize being the largest there is a drop in peak load.

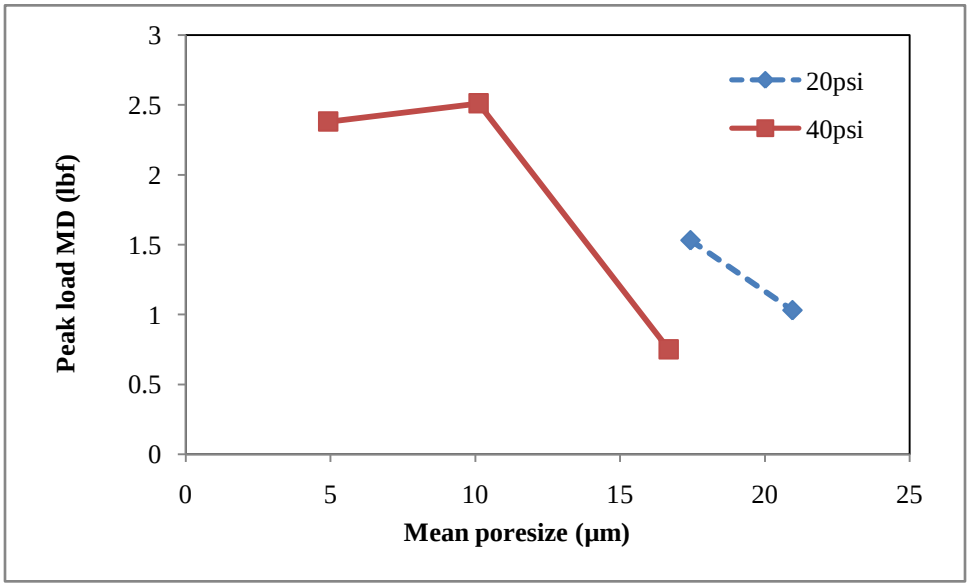

Figure 4-16. Peak load (lbf) vs. mean poresize (µm) of PBT MB substrates.

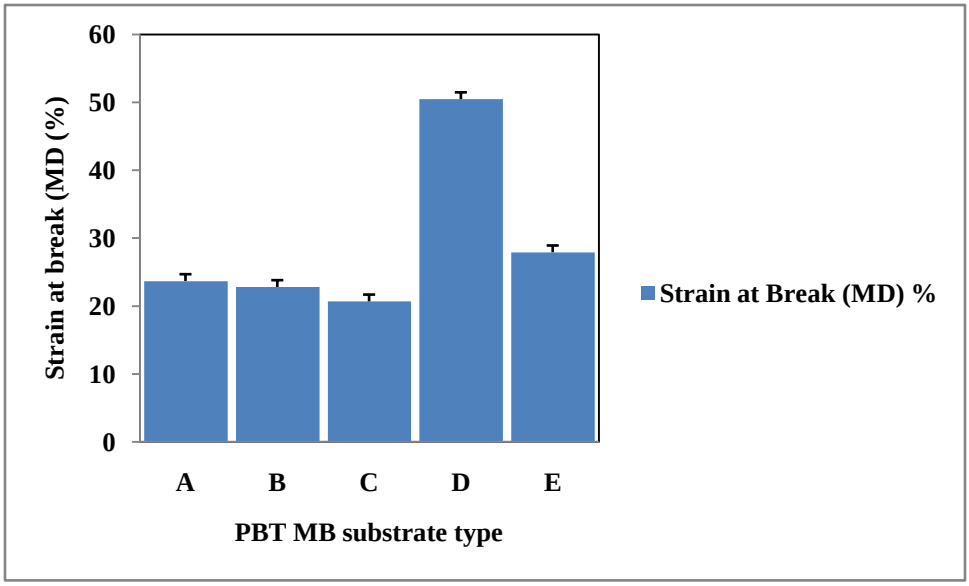

Figure 4-17. Strain at break(%) for PBT MB substrates A, B, C, D and E.

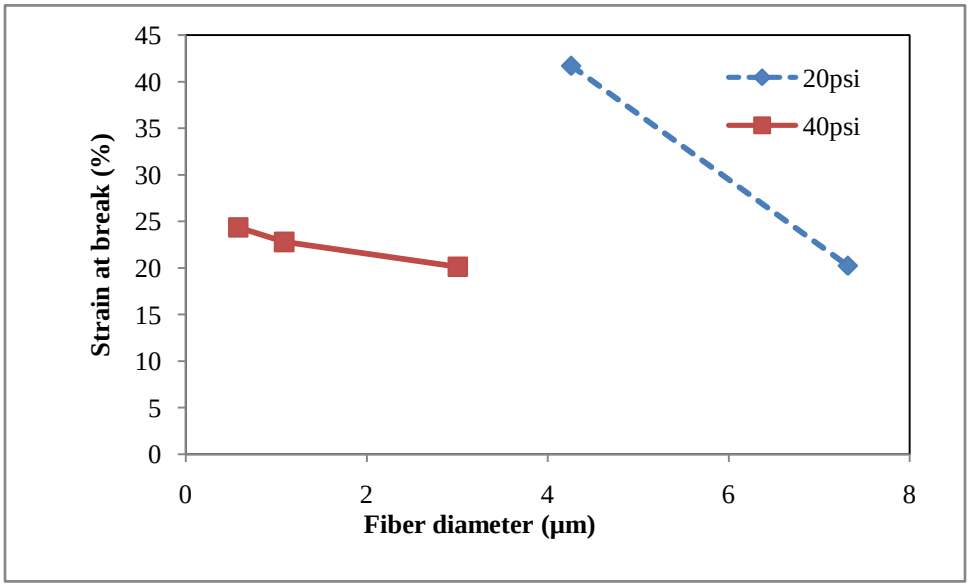

Figure 4-18. Strain at break (%) vs. mean fiber diameter (µm) for PBT MB substrates A, B, C, D and E.

4.2. Characterization poly(butylene terephatalete) (PBT) meltblown substrate grafted with Glycidal methacrylate (GMA) and Dimethylamine (DEA): Process-Structure -Property Relationship

4.2.1. Observations made through SEM Micrographs post GMA treatment of PBT MB substrates

Treated and untreated webs were observed using the SEM for indications of known GMA grafting characterstics. Carbonell et. al. has extensively researched surface modification of meltblown substrates (PP and PBT), his group has worked towards achieving conformal grafting layers of hydrophilic neutral material with functional groups around a hydrophobic fiber to eliminate non-specific protein binding and to maintain porosity of the substrate. They have done so by studying polymerization variables such as polymerization time, monomer-initiator concentration and UV intensity with respect to intrinsic surface area that MB substrates provide.

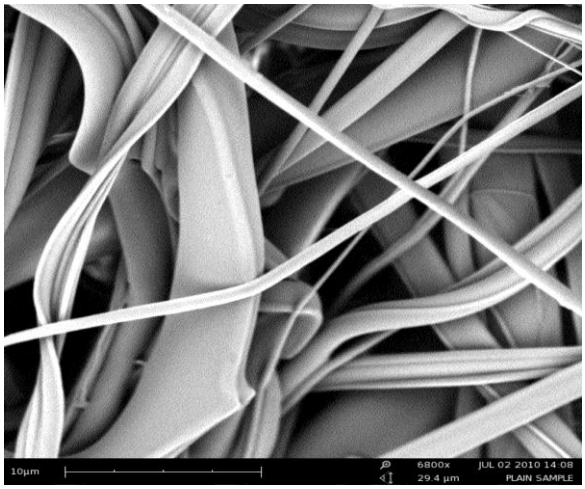

Figure 4-19. SEM micrograph of untreated PBT MB nonwoven substrate.

In Figure 4.19 , SEM micrograph of untreated PBT MB nonwoven substrate shows a smooth surface , varying fiber diameters and fiber shape. The GMA polymerization takes place on the surface of the fiber to produce a polyGMA.

In this research we have used a simple two step grafting technique indicated by Zheng and Liu (3) all polymerization variables were identical for all five substrates A, B, C, D and E. It was observed through SEM micrographs in Figure 4.20 that as the mean fiber diameter increases the grafted surface looks visually less conformal. It can be supposed in this case that as the fiber mean diameter increases from substrate A to E, the surface area decreases and due to this, there is lesser intrinsic surface area available for polymerization to take place, resulting in clumps or 'mushroom' formation of brushes on the surface of the fibers the details of such polymer formation during grafting has been mentioned in Section 2.4.4.

For substrate A, the grafting seems almost conformal, this was observed in several micrographs. In comparison to substrate A the surface of substrate E post GMA grafting is in not as conformal. It can further be observed, that the porosity of the substrate has been maintained in all. It can be seen in the SEM micrograph of substrate A below, that the fiber surface is covered by a textured film, consisting of polyGMA grafts.

For I:M of 1:25 similar observations have been made of PP MB substrate (3). The only difference between the grafted and original fiber (Figure 4.9 and Figure 4.20) is that the fiber surface is covered with conformal undulating polyGMA grafts.

In case of substrates B, C, D and E the grafting is more irregular. It can also be said that the intrinsic surface area of the fiber increases due to the formation of polyGMA ‘mushroom’. To be able to correctly evaluate, protein binding capacity vs. intrinsic surface area of fiber, it would be necessary to target achieving conformal coating for all substrates.

A.

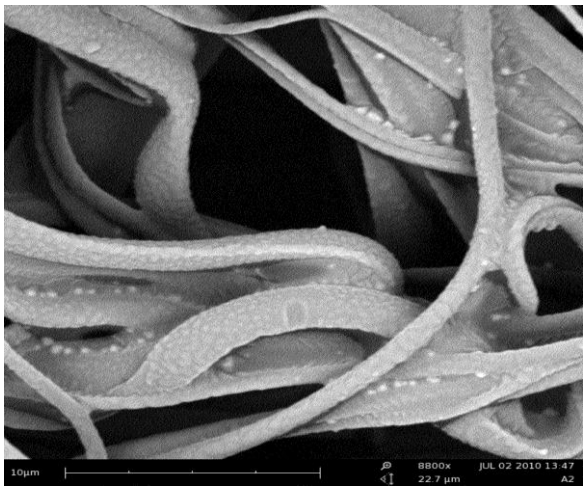

B.

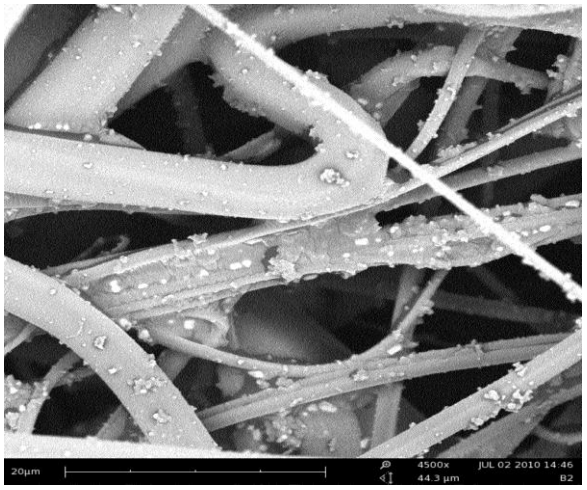

Figure 4-20. SEM micrographs of polyGMA grafted PBT MB nonwoven substrate. Mean fiber diameter of nonwoven substrate A. 0.84µm, B. 1.58µm

C.

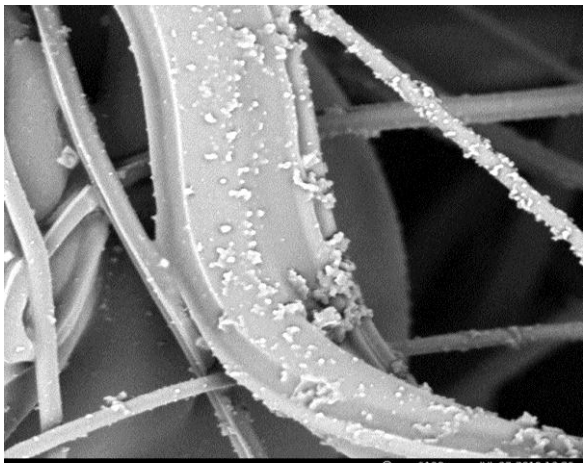

D.

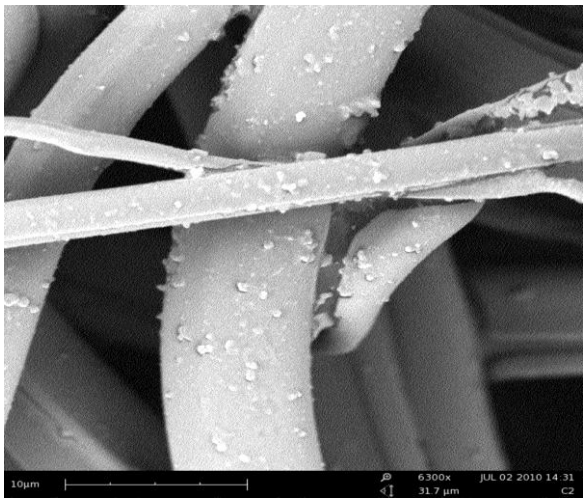

E.

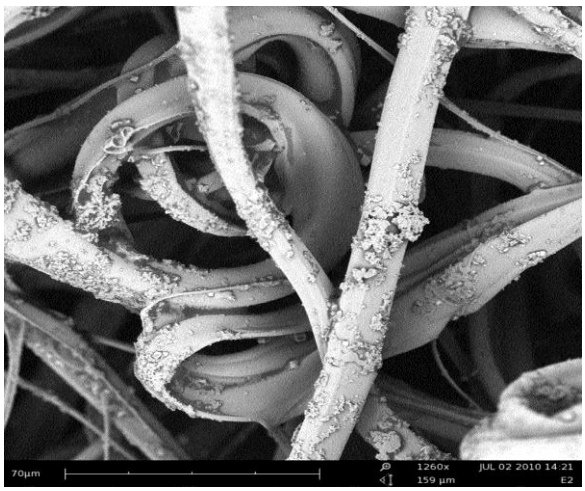

Figure 4-20. SEM micrographs of polyGMA grafted PBT MB nonwoven substrate. Mean fiber diameter of nonwoven substrate C.3.16µm D.4.32µm , E.7.56µm

4.2.2. Weight gain analysis of GMA-DEA treated PBT MB nonwoven substrate

In Figure 4.21 it can be observed that the general trend indicated is, as the fiber diameter increases the weight gained post GMA grafting and DEA treatment decreases, a similar trend can be observed for substrate A, B, C, D and E.

However, for substrate C it is observed that there is a structure-property apart from fiber diameter influencing weight gain (%). The weight gain (%) of substrate C is the least when compared to substrate A, B, D and E as noted in Figure 4.22. For all substrates produced with 40psi air pump pressure i.e. A, B and C the wt. gain and fiber diameter relationship is almost linear, however the overall trend suggests a non-linear graph.

Table 4.7 PBT MB substrate A,B,C,D and E weight gain (%) post GMA and GMA-DEA treatment

Sample ID for PBT MB	A	B	C	D	E
Basis weight (gsm)*	55±1	55±3	55±4	55±4	55±10
Mean fiber diameter(µm)	0.84	1.58	3.16	4.32	7.56
Wt. Gain Post GMA Grafting (%)	11.21	6.04	1.45	4.28	3.48
Wt. Gain Post GMA-DEA (%)	14.15	8.89	2.8	5.73	5.03

Sample size: *Std. Dev. of 6 samples was considered

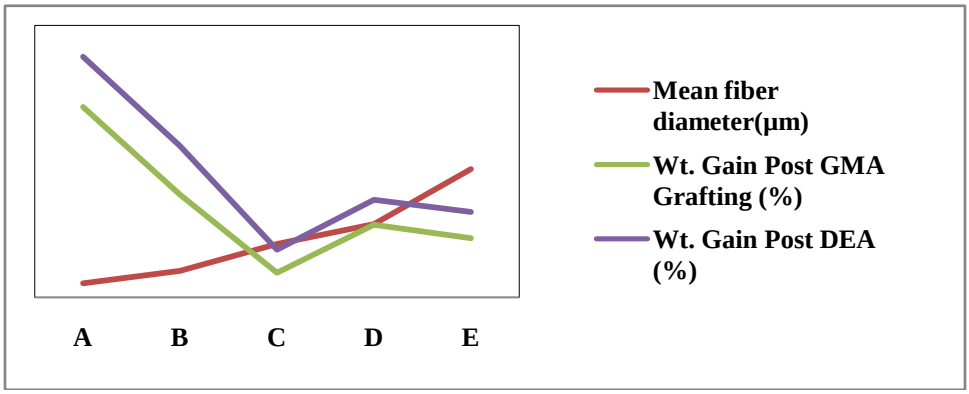

Figure 4-21. Wt. gain (%) and mean fiber diameter (µm) trend for PBT MB substrate A, B, C, D and E.

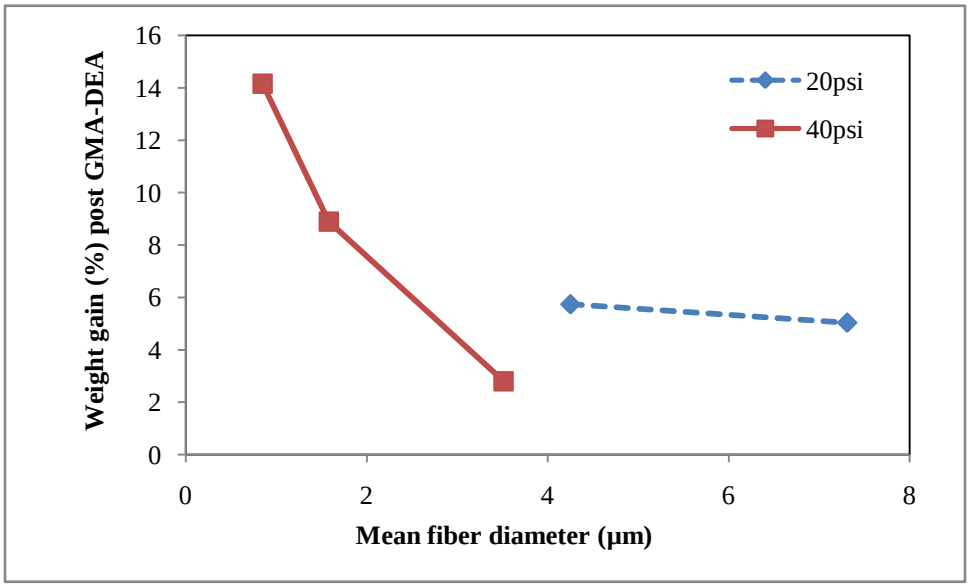

Figure 4-22. Wt. gain (%) vs. mean fiber diameter (µm) curve for PBT MB substrate A, B, C, D and E.

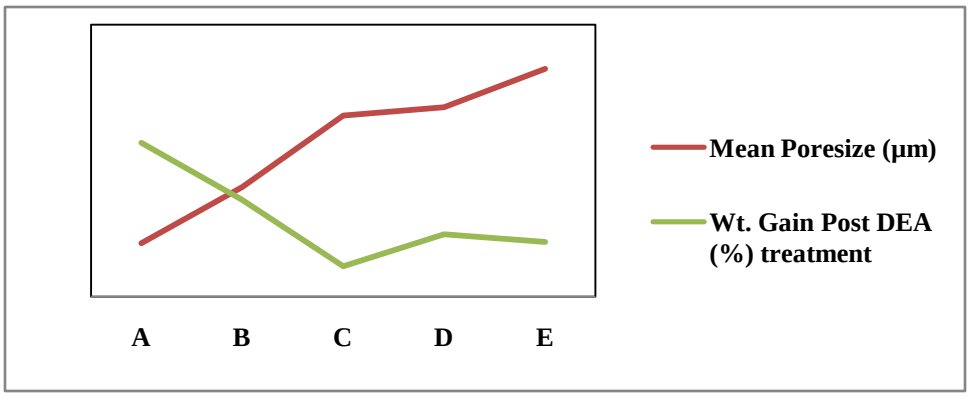

Figure 4-23. Mean poresize (µm) and wt. gain (%) trend for PBT MB substrate A, B, C, D and E.

In Figure 4.23 it can be observed that with the increase in the mean fiber diameter of the substrates from A to E the weight gain (%) decreases gradually. Weight gained by substrate A,B,C,D and E during grafting is influenced by fiber diameter and 'poresize'.

To support this idea it can be observed in Figure 4.23 and Figure 4.24 that the mean pore size of the substrates and the weight gained by them post GMA-DEA treatment display a linear inverse relationship for substrate A, B and C. However for substrate D and E this is not the case.

An understated factor that greatly influences the equilibrium binding capacity of the substrates is the mean pore size. Hence, while the fiber diameter increases relatively gradually from substrate A to E , the weight gain seems to be influenced by both the poresize and the fiber diameter.

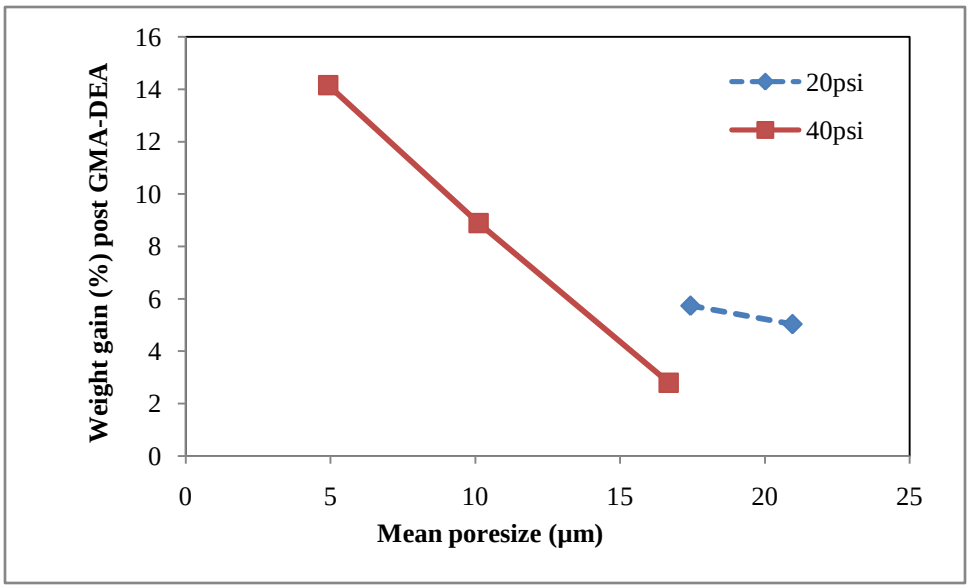

Figure 4-24. Wt. gain (%) vs. mean pore size (µm) for PBT MB substrates A,B,C,D,E.

In the case of substrate C and substrate D, the mean poresize is nearly the same, as noted in Figure 4.23, while the fiber diameter increases constantly, suggesting that for substrate C the mean fiber diameter is small and the pore size comparative larger in proportion to the mean fiber diameter and poresize ratios of other substrates. Overall trends suggest weight gain and fiber diameter is inversely related.

4.2.3. Tensile Strength Analysis of GMA-DEA treated PBT MB nonwoven substrate

Polyesters such as PET and PBT are known to degrade when exposed to UV and high concentrations of bases, in the case of the two step grafting (3) , the PBT MB substrate A,B,C,D and E are exposed to first photografted with polyGMA brushes and then are further treated with DEA which is a base, to convert brushes into an anion exchanger.

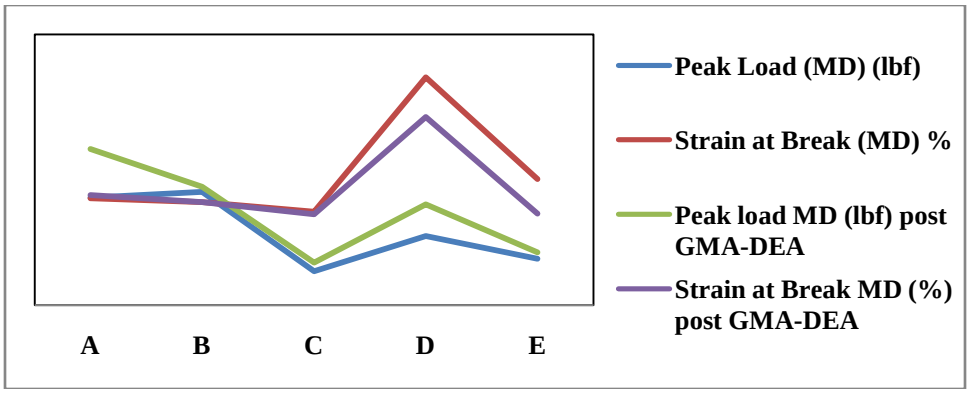

Figure 4-25. PBT MB substrate tensile property comparison before and after GMA-DEA treatment of A,B,C,D and E.

The general trend in Figure 4.25 suggests that in all cases the substrate A,B,C,D and E tensile property improve post GMA-DEA treatment, peak load (lbf) for substrates A to E are higher. This is especially noticeable in the case of substrate A and substrate D, where the peak load (lbf) is much improved after GMA-DEA treatment, this could be due to the fact that the post treatment weight gain for substrate A has been the maximum. Factors influencing tensile property after GMA-DEA treatment are to do with the structure of the substrate, since the coating on the fibers seem to improve the integrity of the substrates, contributing to the strength of the fabric. For substrate A, where maximum number of fibers lie in the bin(0-1) (Figure 4.3 A) the weight gain is maximum, since the intrinsic surface area is maximum, however, tensile strength improves due to the fact that fiber-fiber binding and interaction improves with smaller fiber diameters. In Figure 4.26 and Figure 4.27 it can be observed that peak load (lbf) for substrate C is the lowest and the strain at break (%) for substrate D is the highest.

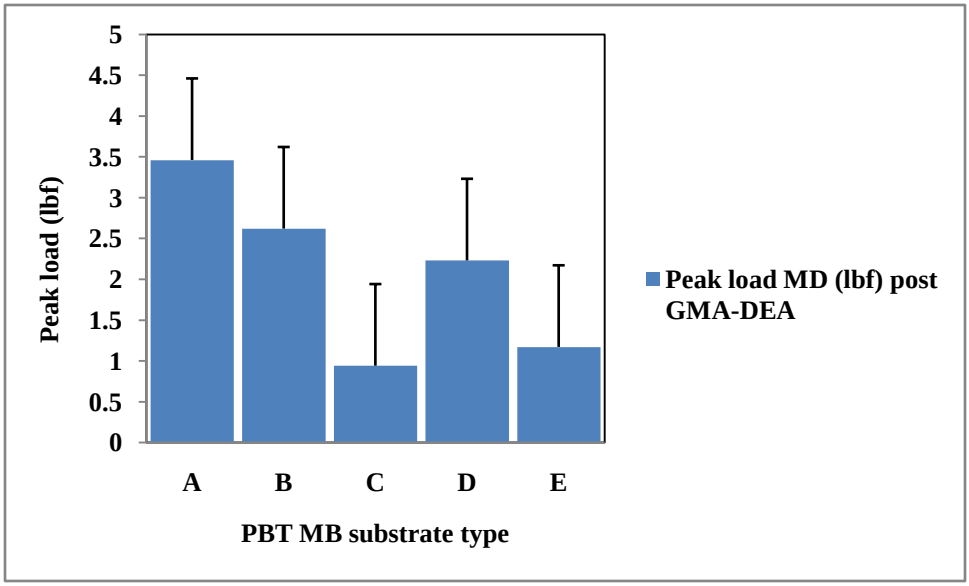

Figure 4-26. PBT MB substrate A,B,C,D and E peak load (lbf) post GMA-DEA.

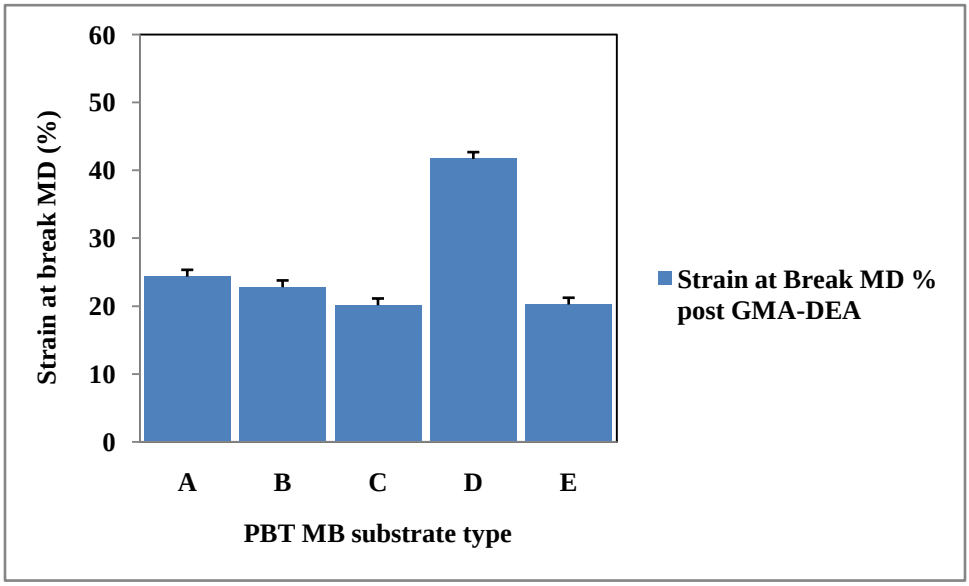

Figure 4-27. PBT MB substrate A,B,C,D and E strain (%) post GMA-DEA.

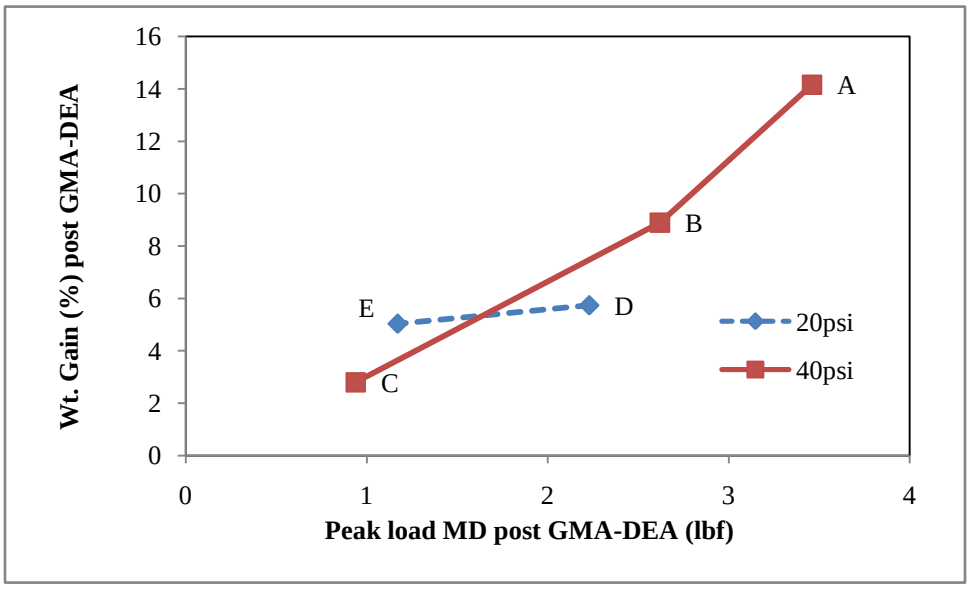

Figure 4-28. Peak load(lbf) and wt. gain (%) of PBT MB substrate A,B,C,D, and E post GMA-DEA.

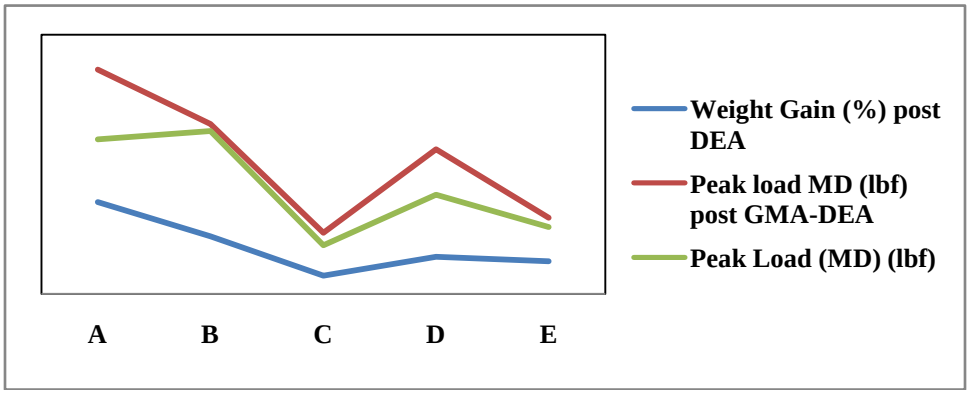

Figure 4-29. PBT MB substrate A,B,C,D and E Peak Load (lbf) post GMA-DEA.

In Figure 4.22 as the mean fiber diameter of the substrates seen to increase from A to C, a corresponding drop is observed in weight gain (%) ,while the peak load (lbf) trend is similar to that of weight gain (%) .

In Figure 4.28 the A and D have higher peak load post wt. gain this is because, fiber-fiber interaction post weight gain is greatly improved for these two substrates.

4.2.4. FTIR spectroscopy of GMA-DEA grafted PBT MB nonwoven substrate

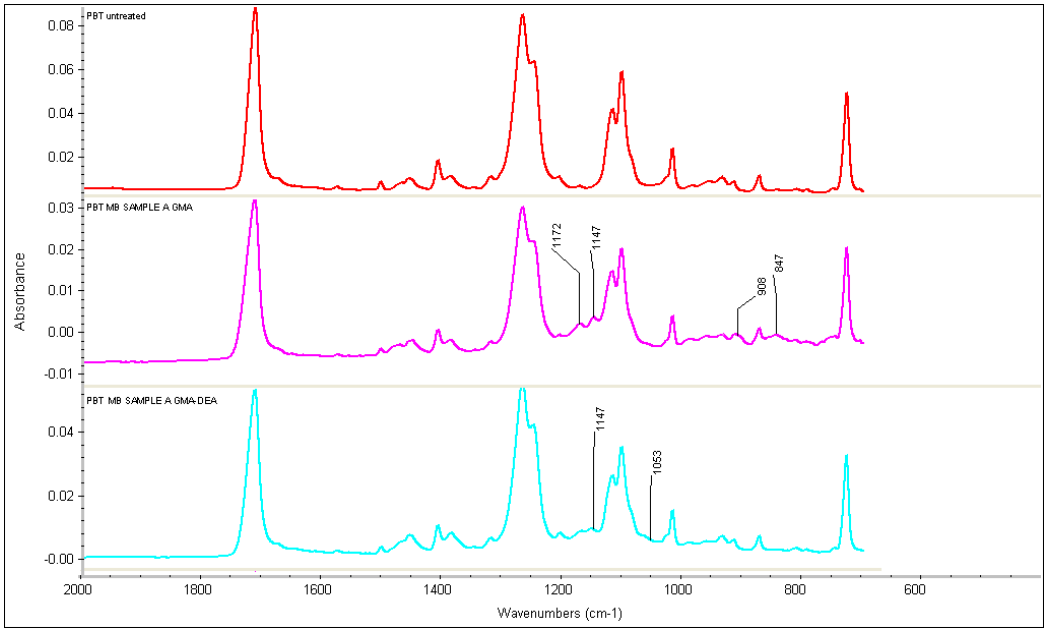

Figure 4-30. FTIR spectra of PBT before and after treatment with GMA-DEA.

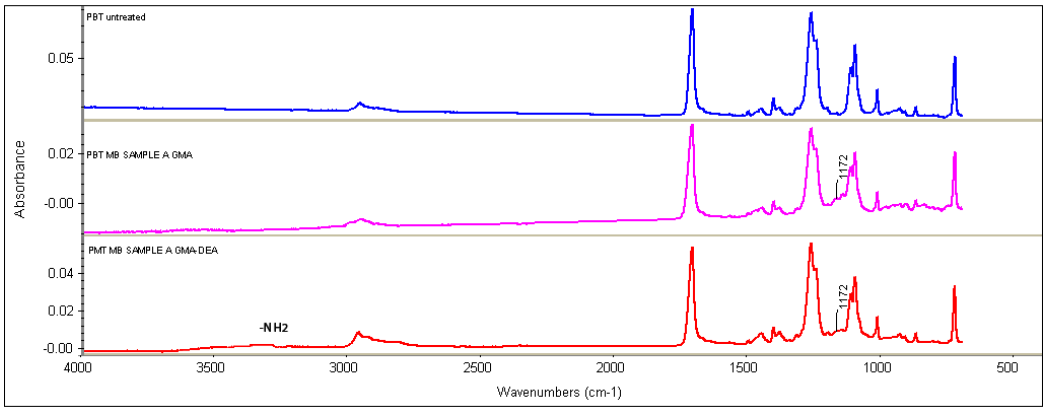

Figure 4-31. FTIR spectra of (a) blank PBT (Blue)(c) PBT polyGMA(Pink) (d) PBT GMA-DEA(Red).

When PBT is treated with GMA these should be an increase in C(O)-OC (carboxyl peaks) and an increase in C(O)-C (epoxy peaks).Peaks at 1172cm^{-1} and 1147cm^{-1} in the PBT GMA treated sample show the increase of carboxyl group C(O)-OC. Epoxy peaks at 847 and 908cm^{-1} in the grafted PBT sample are clear indications of polyGMA grafts. Further when PBT polyGMA is treated with DEA, the content of carboxylic groups is suppose to rise , while the epoxy content is suppose to drop since amine groups attach to the epoxy in polyGMA. This is also affirmed in the FTIR spectrum of the PBT GMA-DEA treated samples. Tertiary amine groups are suppose to show as indicated in ~1060cm^{-1}. As (-OH) groups are added, these can be observed at 3400 cm^{-1}. There is a relative decrease in the peaks at 1172cm^{-1} and 1147cm^{-1} for carboxyl, however epoxy peaks at 847 and 908cm^{-1} are notably reduced as expected. The overall spectrum for PBT GMA-DEA does not show a pronounced (-NH $_2$) peak, suggesting that the treatment of PBT MB samples at 20%(v/v)

DEA solution at 25ºC for 5.2 hrs may not be adequate. However, there is a compromise to be made between substrate strength and the choice of treatment conditions, effects of UV and alkali treatment on polyester has been discussed in Section 2.1.

4.3. Protein adsorption analysis of Glycidal methacrylate (GMA) and Dimethylamine (DEA) grafted Polybutylene Terephatalete (PBT) meltblown substrate.

Analysis of equilibrium protein binding capacity was done using two instruments:

- **HPLC**
- **AKTA Purifier**

The advantages of both instruments has been described in Section 2.6.2. of the literature review, however, the major advantage is lies in the different in flow rates that can be achieved. With the HPLC , low flow rates are achievable i.e. 0.5 ml/min and 0.08 ml/min, where as with the AKTA purifier flowrates as high as i.e. 1ml/min to 4ml/min. are achievable In this research, we have explored both, so as to observe the effect of high and low flowrate on the PBT MB anion exchange substrates.

4.3.1. High Protein Liquid Chromatography (HPLC)

4.3.1.1. Analysis of PBT MB structure property relationship and Protein adsorption

For each of the five GMA-DEA treated PBT MB substrate A, B, C, D and E, Millipore™ columns were packed separately with 30 layers of 1.1 cm diameter disks. After packing the column thickness was measured. The data below in Table 4.8. has been calculated for accumulated properties of all 30 layers post packing, where all the layers are being treated as one layer.

Table 4.8 Cumulative and Independent properties of PBT MB substrates

Cumulative properties (30 layers)	A	B	C	D	E
GSM (30 layers) (g/m^2)	1967	1806	1722	1731	1784
Solidity (30 layers)	0.45	0.40	0.30	0.40	0.37
Protein (mg)/gram fiber @0.08 ml/min	9.081	4.754	1.79	3.988	4.479
Protein (mg)/gram fiber @ 0.5 ml/min	7.587	3.178	1.665	3.273	3.12
Weight gain (%)	14.15	8.89	2.80	5.73	5.03
Independent Properties	**A**	**B**	**C**	**D**	**E**
Mean Fiber Diameter (µm)	0.84	1.58	3.16	4.32	7.56
Intrinsic Surface area/g fiber (m^2/g)	3.60	1.90	0.90	0.67	0.38
Weight gain (%)	14.15	8.89	2.8	5.73	5.03

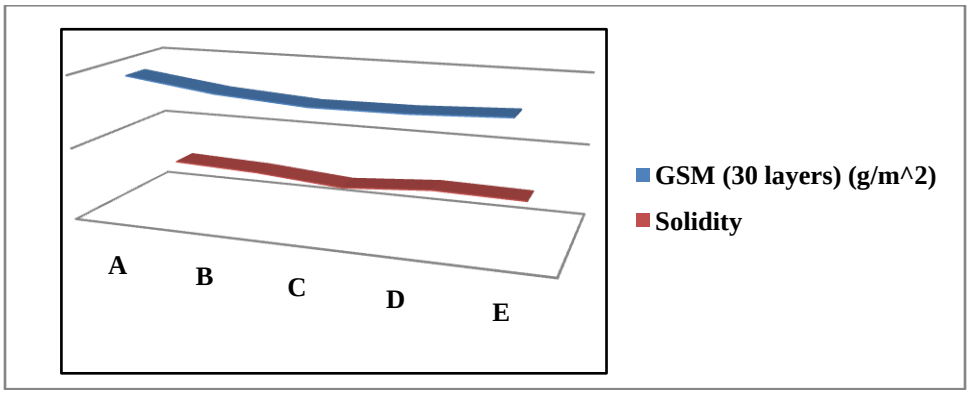

Figure 4-32. Post packing solidity and basis weight of substrate A, B, C, D and E post GMA-DEA treatment.

Post packing, it can be noted in Figure 4.32, that columns A,B,C,D and E show little variation in solidity while the cumulative basis weight is a little higher for substrate A and B this is due to weight gained by the substrates post GMA-DEA treatment.

For substrate C, both solidity and basis weight post packing show a deviation from trend, this can be accounted for by the fact the substrate C has large poresize and comparatively smaller mean fiber diameter when compared to substrate D and E.

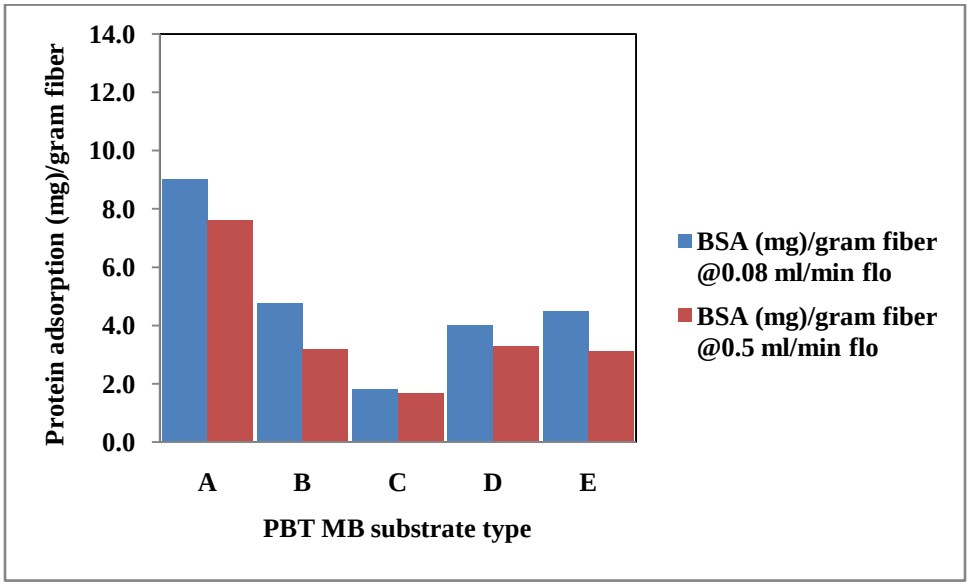

Figure 4-33. Protein adsorbed (mg) per gram fiber at flowrates of 0.08 ml/min and 0.5 ml/min (HPLC).

In Figure 4.33 it can be observed that equilibrium protein binding capacity (discussed in Section 2.6.2) of substrate A is the highest, while substrate C has the lowest value, this can be accounted for by the fact, that the weight gain post GMA-DEA treatment of substrate A is the highest (aprox.14 %) where as the weight gain post GMA-DEA treatment of substrate C is the lowest (aprox.3%) when compared to all other substrates. Discussion on weight gain by GMA-DEA treated substrates A, B, C, D and E has been covered elsewhere in the document (Section 4.2.2) however, poresize and fiber diameter were observed as the major influencing factor.

Substrate A has the smallest mean fiber diameter and pore size , while for substrate C there is a deviation observed from trend for mean pore size, the mean pore size is similar to that of substrate D and E, however the fiber diameter is relatively smaller in comparison. Mean poresize cannot directly be related to equilibrium protein binding capacity, since poresize for 30 layers of substrate was not measured , but wt. gain of substrates can be directly related to poresize. Substrate C is seen to have both low weight gain and protein binding capacity.

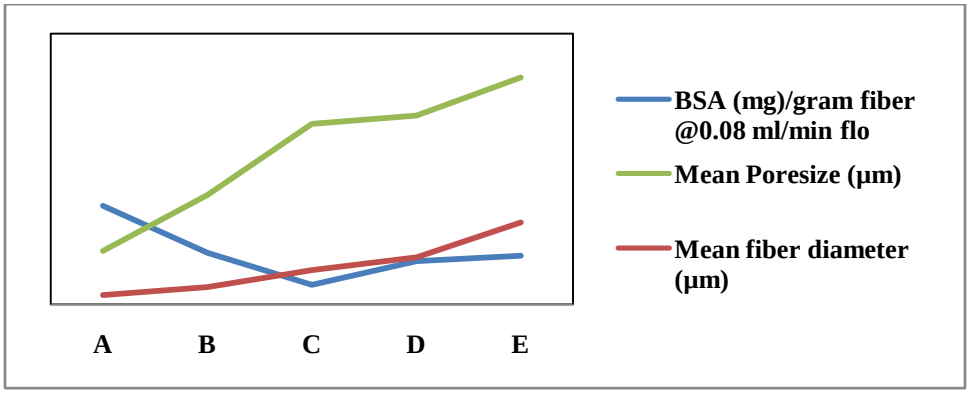

Figure 4-34. PBT MB substrates A,B,C,D and E trend for equilibrium protein binding capacity at 0.08ml/min flow, mean poresize and mean fiber diameter (HPLC).

It can be noted through Figure 4.34 that for substrate D, the slight deviation in trend observed for mean fiber diameter and small rise in the mean pore size is reflected in increased BSA protein binding capacity of the substrate. In Figure 4.36 it is seen that the weight gain trend and BSA protein binding capacity for substrate A,B,C,D and E are similar. The protein binding capacity of the PBT MB substrates is influenced by weight gain (%) and poresize distribution. Weight gain (%) is influenced by fiber diameter and poresize of the substrates.

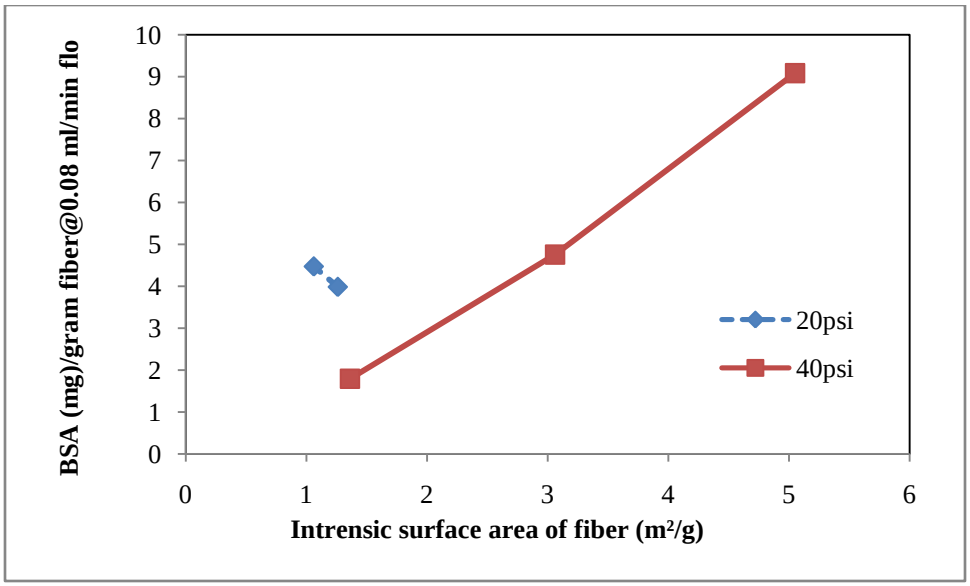

Figure 4-35. PBT MB substrates A,B,C,D and E equilibrium protein binding capacity at 0.08ml/min flow vs. intrinsic surface area (HPLC).

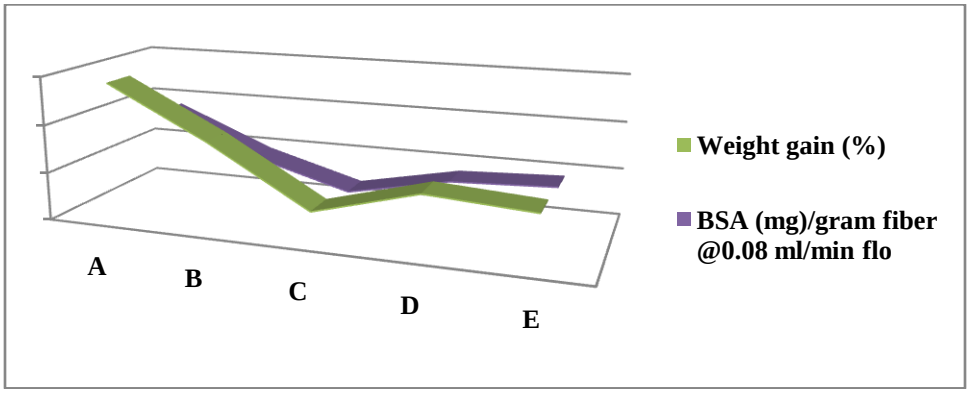

Figure 4-36. PBT MB substrates A,B,C,D and E displaying similar trend for Wt. gain (%) and protein adsorption (mg) per gram fiber at 0.08 ml/min flow rate (HPLC).

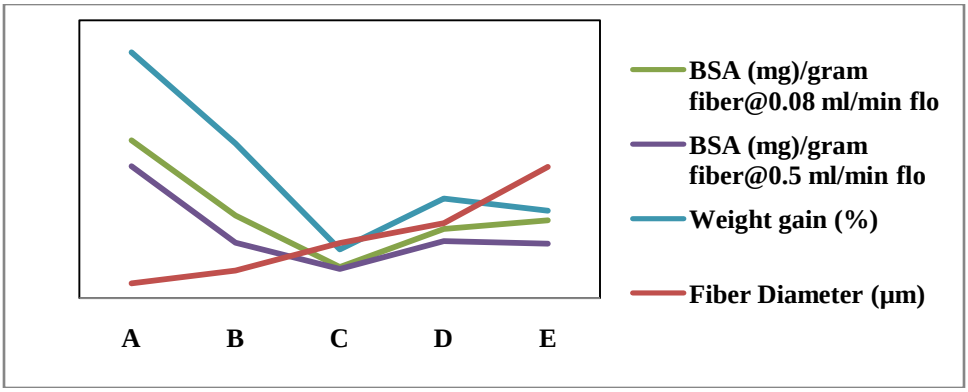

Figure 4-37. PBT MB substrate A,B,C,D,E trends for (a) equilibrium binding capacity at flow rates 0.08 ml/min and flow rate 0.5ml/min (HPLC) (b) Wt. gain (%) post GMA-DEA treatment and (c) Fiber diameter (µm)

In Figure 4.37 the general trend suggests that as the mean fiber diameter increases the BSA protein binding capacity decreases. Deviation from trend is observed for substrate C, the reasons observed are increased pore size and decreased fiber diameter when compared to substrate D and E.

Figure 4.38 illustrates trends of substrate A,B and C, all three substrates have only one production variable i.e. throughput (ghm), while their production air velocity is the same. It can be observed that if the production variable of 'air velocity' is kept constant i.e. substrates A,B and C were produced at 40psi air pump pressure, then weight gain (%), fiber diameter and BSA protein binding capacity, all reflect the theoretical concept that, as the intrinsic surface area of the substrate increases the BSA protein binding capacity increases. By keeping constant 'air velocity' during production, we may have eliminated one of the causes for change in poresize distribution trend observed for substrate C.

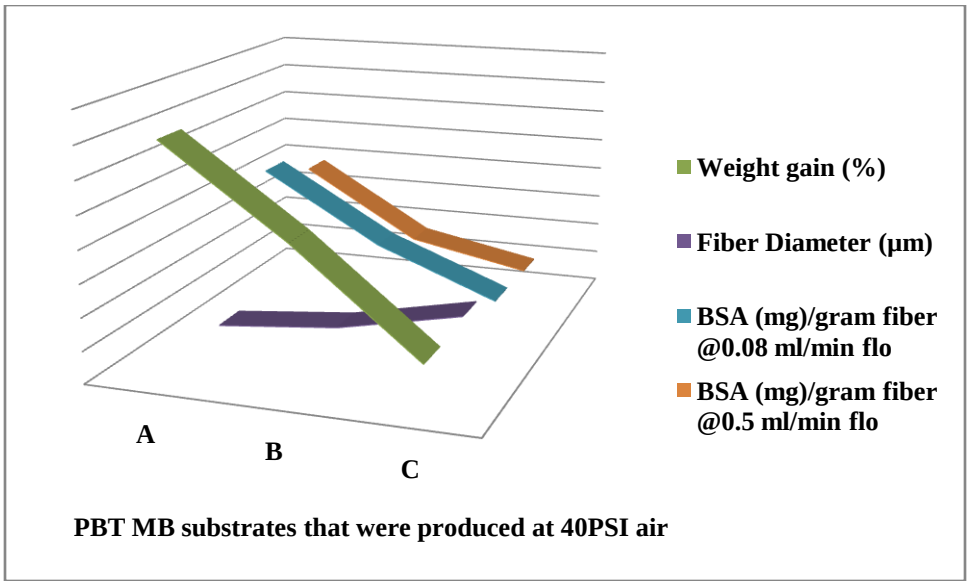

Figure 4-38. PBT MB substrate A,B,C trends for (a) equilibrium binding capacity at flow rates 0.08 ml/min and flow rate 0.5ml/min (HPLC) (b) Wt. gain (%) post GMA-DEA treatment and (c) Fiber diameter (µm).

4.3.1.2. Analysis of PBT MB structure-property relationship and flowrate

A common trend observed in Figure 4.39 is that as the flowrate increases the equilibrium protein binding capacity of the GMA-DEA substrate A,B,C,D and E decreases, showing a direct dependence of equilibrium protein binding capacity on flowrate. Substrate B, D and E nearly have the same equilibrium binding capacity at 0.5 ml/min flowrate, suggesting that at a higher flowrate than 0.5ml/min the equilibrium binding capacity of these three substrates becomes independent of flowrate. This observation is further confirmed when we study equilibrium protein binding of GMA-DEA grafted substrates A,B,C,D and E at higher flowrates on the AKTA™ FPLC purifier.

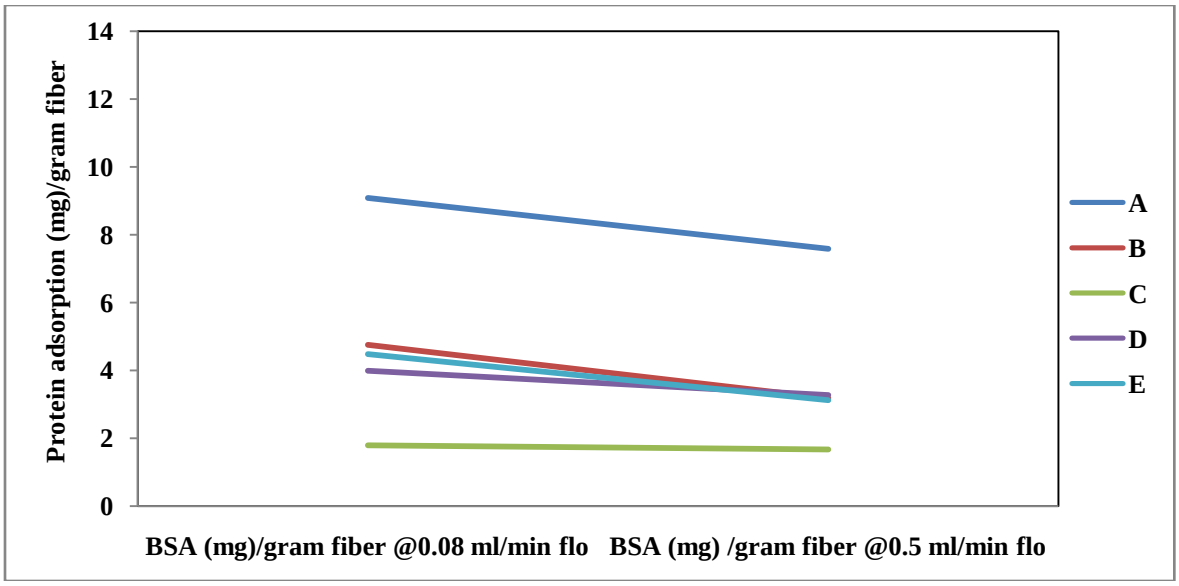

Figure 4-39. PBT MB substrates A,B,C,D and E display equilibrium protein binding capacity at flow rates of 0.08 ml/min and 0.5 ml/min (HPLC)

Substrate C has least response to the change in flowrate (as discussed in Section 2.3.2), the equilibrium protein binding capacity remains nearly the same as flowrate increases from 0.08ml/min to 0.5ml/min. While in the case of substrate A, possibility of 'diffusion' as a filtration mechanism can be considered a reason for higher protein binding, due to its small poresize, this phenomenon becomes more pronounced at lower flowrates. Substrates B, D and E also illustrate better diffusion as well as adsorption characterstics at lower flowrates (i.e. diffusion and adsorption is the reason for higher equilibrium protein binding capacity at lower mobile flowrates) however, as the flowrate increase from 0.08ml/min to 0.5 ml per min principles of diffusion become limited since the mobile phase flows through the substrate preferably through the larger pores, i.e. the path of least resistance.

While in the case of substrate A, the mean pore size is much smaller (aprox.~3µm) hence even at higher flowrates, the mobile phase is forced through relatively smaller pores.

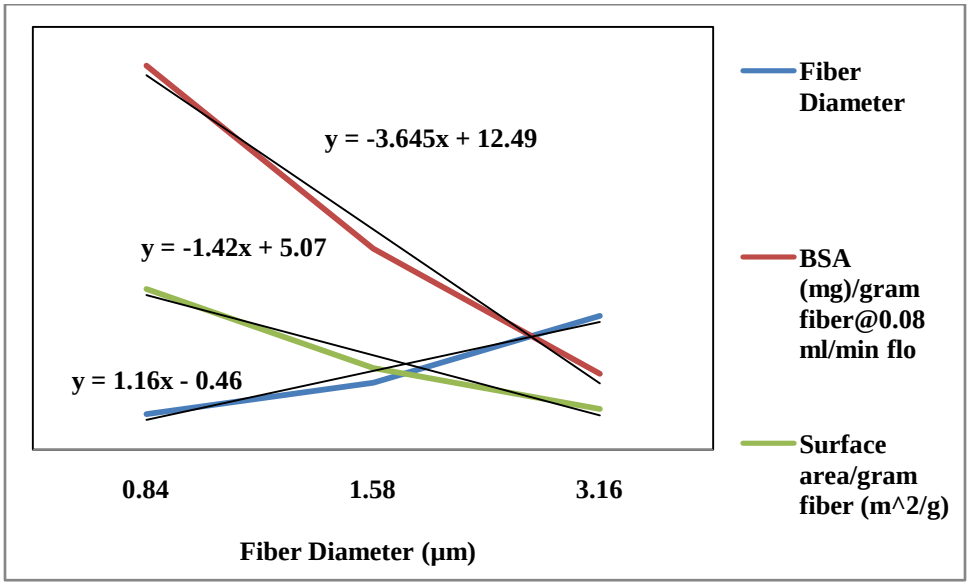

Figure 4-40. Fiber diameter, fiber surface area and equilibrium protein binding capacity (0.08ml/min flowrate) for PBT MB substrates A, B and C, these substrates were all produced at 40psi air pump pressure.

4.3.2. AKTA PURIFIER

4.3.2.1. Analysis of PBT MB structure property relationship and equilibrium protein binding capacity of substrates A,B,C,D and E

For each of the five GMA-DEA treated PBT MB substrate A, B, C, D and E, Millipore™ columns were packed separately with 90 layers of disks. After packing the column thickness was measured. The data in Table 4.9 has been calculated for accumulated properties of all 90 layers post packing, where all the layers are being treated as one layer.

Table 4.9 Cumulative and Independent properties of PBT MB substrates A,B,C,D and E columns packed for AKTA purifier

Cumulative Properties (90 layers)	A	B	C	D	E
GSM (90 layers)	5421	5397	5094	5215	5196
Solidity	0.221	0.267	0.258	3.41	0.263
BSA (mg)/gram fiber @1ml/min	13.33	7.03	2.48	5.65	3.73
4ml/min (mg)/gram fiber @ 4ml/min	10.91	6.63	2.30	5.13	3.45
Independent Properties (90 layers)	**A**	**B**	**C**	**D**	**E**
Weight gain (%)	14.15	8.89	2.8	5.73	5.03
Fiber Diameter (µm)	0.84	1.58	3.16	4.32	7.56
Surface area/gram fiber (m^2/g)	3.8	1.93	0.96	0.70	0.40

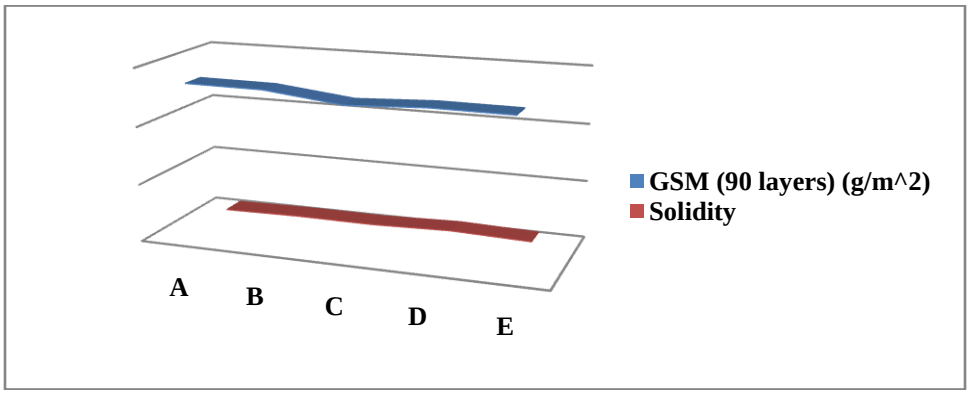

Figure 4-41. Solidity and basis weight for columns packed with substrate A,B,C,D and E post GMA-DEA treatment.

Post column packing, as noted in Figure 4.41, columns A, B, C, D and E show little variation in solidity while the cumulative basis weight is a little higher for substrate A and tends to reduce for substrate E, this is due to weight gained by the substrates post GMA-DEA treatment. Solidity is an important factor while considering flow permeability. For substrate C, basis weight for 90 layers show a deviation from trend, this is due to the fact that weight gained post GMA-DEA treatment is the least.

In Figure 4.42 it can be observed that protein binding capacity of substrate A is the highest while substrate C has the lowest value, this can be accounted by the fact that the weight gain post GMA-DEA treatment of substrate A is the highest (aprox.14%) where as the weight gain post GMA-DEA treatment of substrate C is the lowest (aprox.3%) when compared to all other substrates. This is a similar observation made on protein binding data collected from the HPLC instrument.

Discussion on weight gain by GMA-DEA treated substrates A, B, C, D and E has been covered elsewhere in the document, however, poresize and fiber diameter were observed as the major influencing factor. Substrate A has the smallest mean fiber diameter and pore size while for substrate C there is a deviation observed from trend for mean pore size, the mean pore size is similar to those of substrate D and E however the fiber diameter is smaller in comparison. For substrate E, the equilibrium protein binding capacity is observed to be the least. The overall equilibrium protein binding capacity of the AKTA columns seem to be slightly higher when compared to the HPLC columns, this is because, during protein sample application (AKTA instrument), the BSA loop was 10ml and for the HPLC a 1.5ml loop was used.

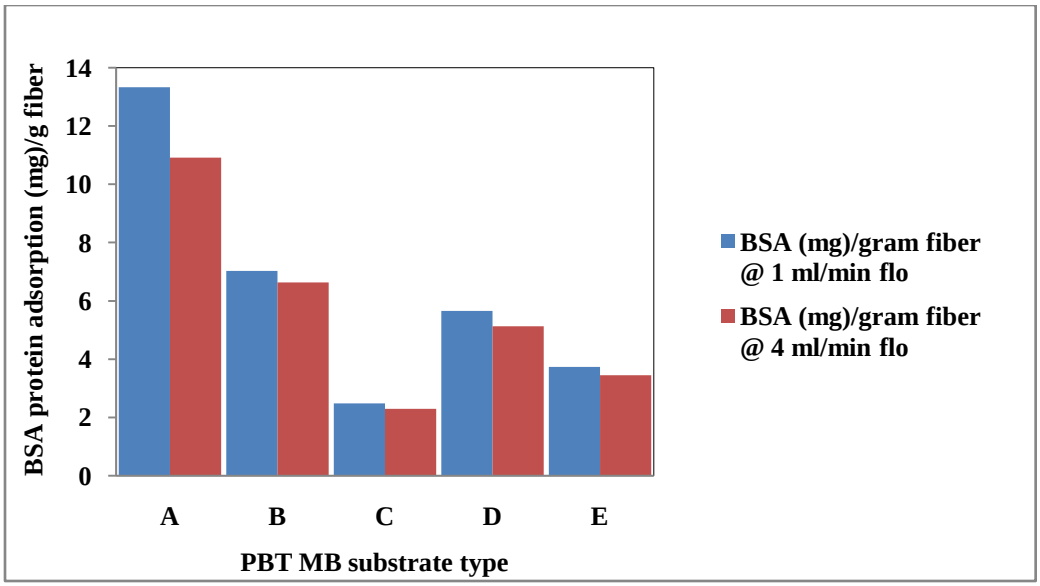

Figure 4-42. PBT MB substrate A,B,C,D and E equilibrium protein binding capacity BSA(mg)per gram fiber at flowrates of 1ml/min and 4 ml/min (AKTA).

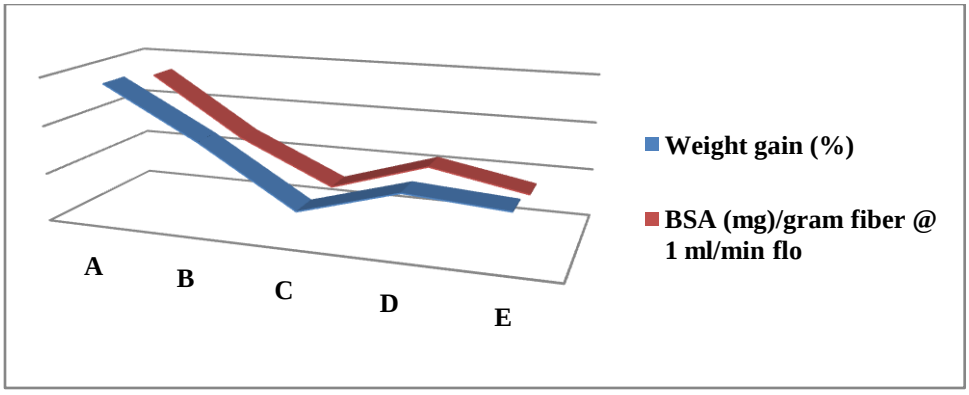

Figure 4-43. PBT MB substrate A,B,C,D and E weight gain(%) and protein binding capacity at 1ml/min flowrate (AKTA).

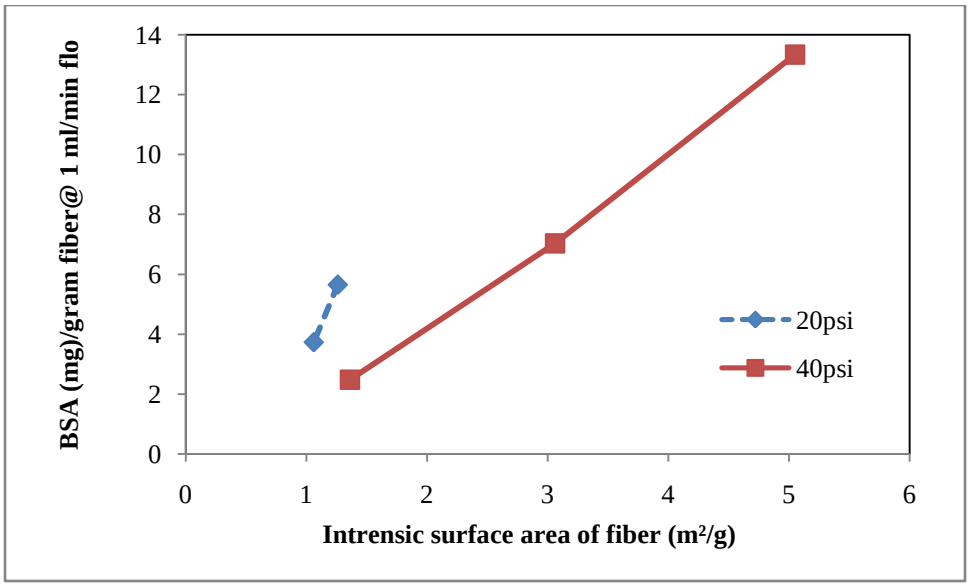

Figure 4-44. PBT MB substrates A,B,C,D and E equilibrium protein binding capacity at 1 ml/min flow vs. intrinsic surface area (AKTA).

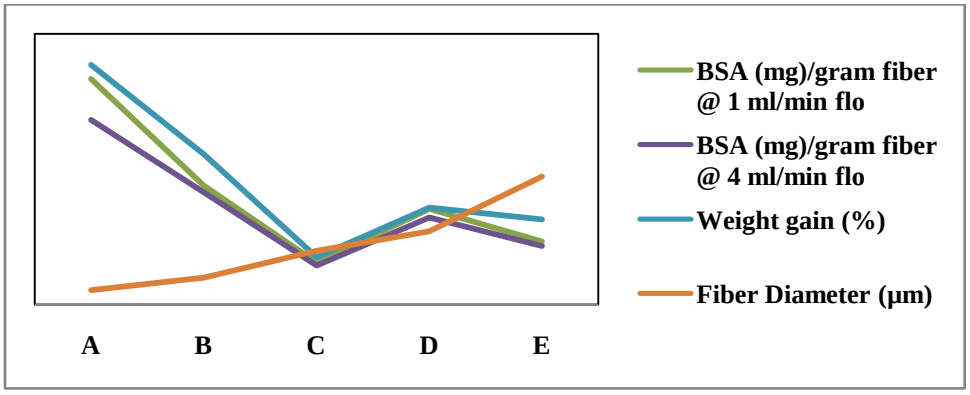

Figure 4-45. PBT MB substrate A,B,C,D,E trends for (a) equilibrium binding capacity at flow rates 0.08 ml/min and flow rate 0.5ml/min (AKTA) (b) Wt. gain (%) post GMA-DEA treatment and (c) Fiber diameter (µm).

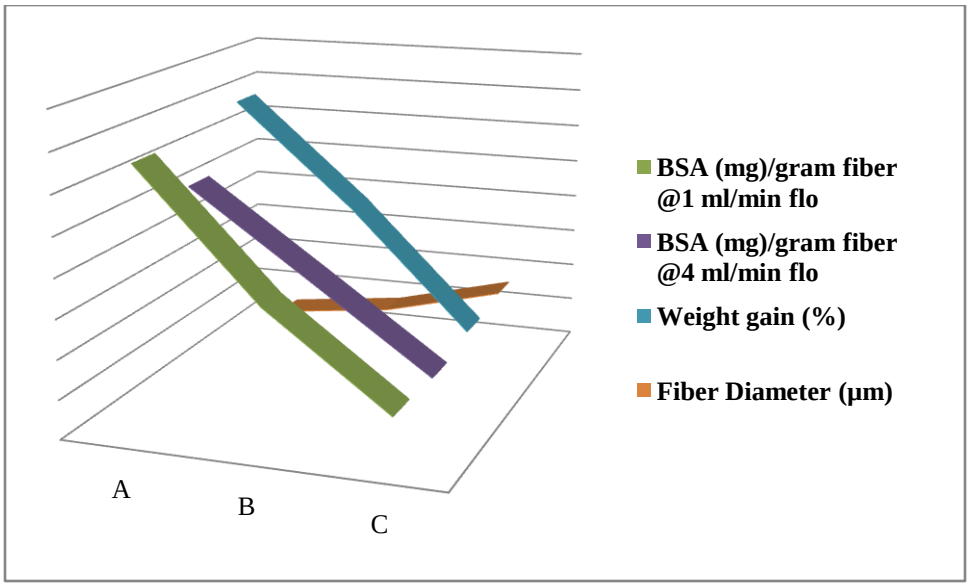

Figure 4-46. PBT MB substrate A,B,C trends for (a) equilibrium binding capacity at flow rates 1 ml/min and flow rate 4 ml/min (AKTA) (b) Wt. gain (%) post GMA-DEA treatment and (c) Fiber diameter (µm).

In Figure 4.45, the general trend is as the mean fiber diameter increases the BSA equilibrium protein binding capacity decreases. Deviation from trend is observed for substrate C, the reasons observed are increased pore size and relative decrease in fiber diameter.

Figure 4.46 illustrates trends of only substrate A, B and C. All three substrates have only one production variable ie. throughput. It can be observed that if the production variable 'air velocity' is kept constant then i.e. substrates A,B and C were produced at 40psi air pump pressure, then weight gain (%), fiber diameter and BSA protein binding capacity, all reflect the theoretical concept that, as the intrinsic surface area of the substrate increases equilibrium protein binding capacity increases. This is true for independent samples A, B and C loaded on the HPLC instrument as well.

4.3.2.2. Analysis of PBT MB structure property relationship and flowrate

A common trend observed in Figure 4.47 is that as the flowrate increases the equilibrium protein binding capacity of the GMA-DEA substrate A,B,C,D and E decreases, showing a direct dependence of equilibrium binding capacity on flowrate.

Substrate B, C, D and E nearly have the same equilibrium binding capacity at 1 ml/min flowrate, suggesting, that at a higher mobile phase flowrate than 4 ml/min the equilibrium binding capacity of these three substrates becomes independent of the effect of flowrate.

In all PBT MB substrates apart from substrate A, which displays possibility of 'diffusion' as a filtration mechanism, that is more pronounced at lower flowrates, the substrate B,C,D and E does not do so due to the increased mean pore size of the substrate.

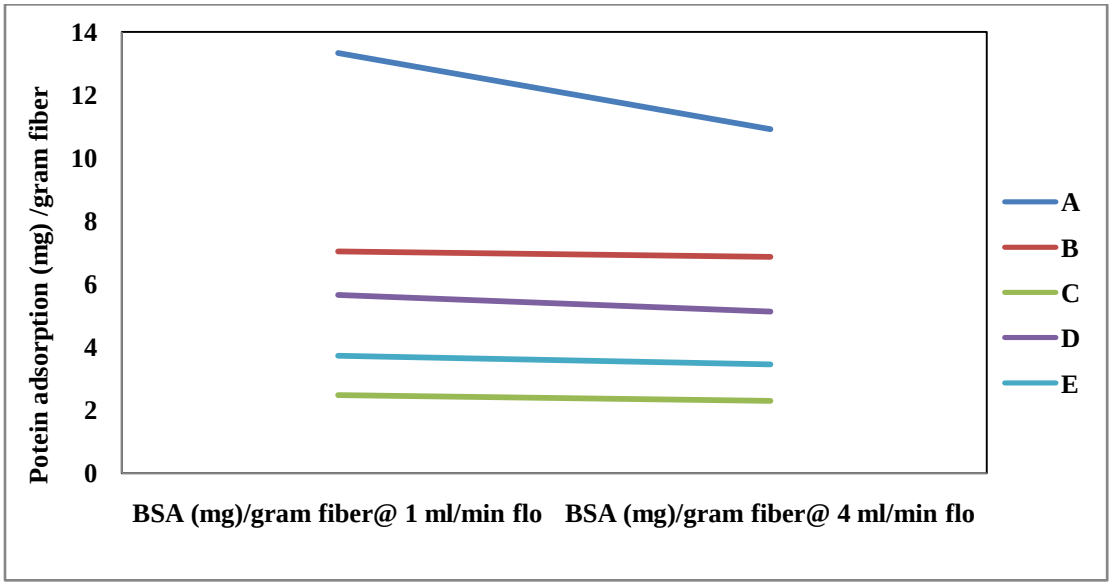

Figure 4-47. PBT MB substrates A,B,C,D and E display equilibrium protein binding capacity at flow rates of 1 ml/min and 4 ml/min (AKTA).

However as the flowrate i.e. 4ml per min , diffusion mechanism have a limiting effect since the mobile phase flows through the substrate takes place through the larger pores, i.e. the path of least resistance (as discussed in Section 2.6.2). While in the case of substrate A, the mean pore size is much smaller (aprox. ~3µm) hence, even at higher flowrates the fluid flow is forced through relatively smaller pores.

.

SECTION 5. CONCLUSION

Meltblown webs of PBT with different fiber diameter distributions were produced by controlling meltblowing processing parameters. The effect of fiber diameter on protein binding capacity of GMA-DEA treated PBT meltblown substrates was investigated in this work.

The first half of the research deals with controlling fiber diameter using process-property relationship (i.e.throughput, air velocity). Mean fiber diameter decreased as polymer throughput decreases at the given air velocity, and increasing air velocity obtained by higher air pressure further reduced diameter of fibers. PBT nonwovens webs with varying fiber diameter distribution ranging from mean fiber diameter of ~0.8μm to that of 7.56μm corresponding intrinsic surface area of ~3.8m^2/g to 0.40 m^2/g, were successfully produced. Reduction of fiber diameter resulted in higher intrinsic surface area and smaller pore size.

During the second part of the research PBT MB substrate with varying fiber diameters distribution were treated with GMA-DEA to investigate the effect of fiber diameter and surface area on GMA grafting reaction efficiency and protein binding capacity. The PBT fiber surface is reacted with GMA monomer in the presence of BP, to produce surface attached poly(GMA), this was further treated with DEA to create an anion exchange medium. In general, the weight gained by different substrates coincides with the increase in intrinsic surface area.

Further PBT MB substrates were evaluate for protein binding capacity, where the protein binding capacity of the PBT MB substrates is influenced by :

- Weight gain (%) and poresize distribution
- The weight gain (%) is influenced by fiber diameter and poresize of the substrate .By keeping constant ‘air velocity’ as a production variable we may have eliminated one of the causes for change in poresize distribution trend of substrate C.
- For ion exchange applications, once flow restrictions reduce, mass transfer limitations become more apparent, especially if the pore size of the membrane is >5µm then mass transfer limitations become rate limiting. The pores of the substrate become so large that the mobile phase flows through the membrane, the protein does not have enough time to bind to the membrane, with little diffusion within the GMA-DEA polymer brushes that are present on the surface of the fibers.

SECTION 6. FUTURE WORK

To be able to correctly evaluate, protein binding capacity vs. intrinsic surface area of fiber, it would be necessary to achieve conformal coating for all substrates.

For substrate grafting conditions, there has to be a compromise made between strength and treatment conditions, it would be advisable to conduct research on what treatment conditions lead to improved tensile properties of the post treated substrates.

Fiber diameter and poresize are both equally important and effect the protein binding capacity of treated substrate, work should be done to understand the influence of poresize on equilibrium protein binding capacity.

REFFERENCES

1. *Influence of pore structure and architecture of photo-grafted functional layers on separation performance of cellulose-based macroporous membrane adsorbers.* **Jun Wanga, Rene Faber, Mathias Ulbrichta.** 1216, 2009, Journal of Chromatography A, pp. 6490–6501.

2. *Alternative bioseparation operations: life beyond packed-bed chromatography.* **Todd M Przybycien, Narahari S Pujar,Landon M Steele.** 15, 2004, Current Opinion in Biotechnology, pp. 469-478.

3. *Polypropylene nonwoven fabrics with conformal grafting of poly(glycidylmethacrylate) for bioseparations.* **Yong Zheng, HaiyanLiu, PatrickV.Gurgel, RubenG.Carbonell.** 2010, Journal of Membrane Science, Vol. 364, pp. 362-371.

4. Ticona. *Ticona.com.* [Online] 2010. http://www.ticona.com/celanex.

5. **Mark J.E., Iroh J.O.** Polymer Data Handbook. *poly(butylene terephthalate).* s.l. : Oxford University Press, Inc, 1999.

6. **Giles H.F., Wagner J.R.** *Extrusion:The definitive processing guide and handbook.* s.l. : William Andrew Publishing, 2005. p. 217. Vol. 1. 0815514735.

7. **Gijsman P., Meijers G.,Vitarelli G.** *Comparison of the UV-degradation chemistry of polypropylene,polyethylene, polyamide 6 and polybutylene terephthalate.* s.l. : Polymer Degradation and Stability, 1999. pp. 433-441. Vol. 65.

8. *Effects of Pretreatment Reagents on the Hydrolysis and Physical Properties of PET Fabrics.* **Kim E.S., Lee C.H.,Kim S.H.** 2009, Journal of Applied Polymer Science, Vol. 112, pp. 3071–3078.

9. *Physical Properties of Polyester Fibers Degraded by Aminolysis and by Alkaline Hydrolysis.* **Ellison M.S., Fisher L.D.,Alger K.W.** s.l. : Journal of Applied Polymer Science, 1982, Vol. 27, pp. 247-257.

10. *The Manufacture of Continuous Polymeric Filaments by the Melt-blowing Process.* **Kayser JC, Shambaugh RL.** s.l. : POLYMER ENGINEERING AND SCIENCE, 1990, Vol. 30.

11. *Meltblowing: I-basic physical mechanisms and threadline model.* **Sinha-Ray S., Yarin A.L.,Pourdeyhimi B.** s.l. : JOURNAL OF APPLIED PHYSICS, 2010, Vol. 108, p. 034912.

12. *Structure and Filtration Properties of Meltblown Polypropylene Webs.* **Lee Y.C, Wadsworth L.C.** s.l. : POLYMER ENGINEERING AND SCIENCE, 1990, Vol. 30, pp. 1413-1419.

13. *A Macroscopic View of the Melt-blowing Process for Producing Microfibers.* **R.L., Shambaugh.** s.l. : INDUSTRIAL & ENGINEERING CHEMISTRY RESEARCH, 1988, Vol. 27, pp. 2363-2372 .

14. *Meltblown structures formed by a robotic and meltblowing integrated system: Impact of process parameters on pore size.* **Velu YK, Ghosh TK, Seyam AM.** s.l. : TEXTILE RESEARCH JOURNAL, 2003 , Vol. 73, pp. 971-979 .

15. **Velu, Y.K.** 3D structures formed by a robotic and meltblowing integrated system. *http://www.lib.ncsu.edu/resolver/1840.16/5490 .* [Online] 2003.

16. *Analysis of a Meltblowing Die: Comparison of CFD and Experiments.* **Krutka H.M, Shambaugh R.L, Papavassiliou D.V.** 2002, Industrial Engineering Chemical Research, Vol. 41, pp. 5125-5138.

17. *The Influence of Power-law Rheology on Flow Distribution in Coathanger Manifolds.* **Reid J.D, Campanella O.H,Corvalan C.M,Okos M.R.** s.l. : POLYMER ENGINEERING AND SCIENCE, 2003, Vol. 43.

18. **Purchas D.B, Sutherland K.** *Handbook of Nonwoven Filter Media.* s.l. : Elsevier Ltd., 2007. ISBN-13:978-1-85617-441-1.

19. www.donaldson.com. *http://www.donaldson.com/en/engine/shoptalk/051978.pdf.* [Online] 2010.

20. http://www.afssociety.org. *http://www.afssociety.org.* [Online] 2010.

21. *The Inertial Mechanism in the Mechanical Filtration of Aerosols.* **Ramskill E.A, Anderson W.L.** THE JOURNAL OF COLLOID SCIENCE, Vol. 6, pp. 416-428.

22. **W.C, Hinds.** *Aerosol technology: Properties, Behavior, and Measurement of Airborne particles.* New York : Wiley, 1999. ISBN 0-471-19410-7.

23. *Mass transfer limitations in protein separations using ion-exchange membranes.* **Sarfert F.T, Etzel M.R.** s.l. : Journal of Chromatography A, 1997, Vol. 764, pp. 3-20.

24. *Improving the flame retardancy of PET fabric by photo-induced grafting.* **Yu L., Zhang S.,Liu W.,Zhu X.,Chen X.** s.l. : Polymer Degradation and Stability, 2010, Vol. 95, pp. 1934-1942.

25. *Surface grafted polymer brushes as ideal building blocks for ‘‘smart’’surfaces.* **Feng Zhou, Wilhelm T. S. Huck.** 2006, Physical Chemistry Chemical Physics, Vol. 8, pp. 3815-3823.

26. **Advincula, Rigoberto C.** *Polymer Brushes: Synthesis, Characterization, Applications.* s.l. : Weinheim Wiley-VCH Verlag GmbH, 2004.

27. *End-Group-Dominated Molecular Order in Self-Assembled Monolayers.* **H. Wolf, H. Ringsdorf.** 1995, Journal of Physical Chemistry, Vol. 99, pp. 7102-7107.

28. *Applications of Polymer Brushes in Protein Analysis and Purification.* **Parul Jain, Gregory L. Baker, and Merlin L. Bruening.** 2, 2009, Annual Review of Analytical Chemistry, pp. 387-408.

29. *Polyelectrolyte-mediated Protein Adsorption.* **Wittemann A., Haupt B.,Ballauff M.** s.l. : Progress in Colloid and Polymer Science, 2006, Vol. 133, pp. 58-64.

30. *Ring-opening reaction of poly-GMA chain grafted onto a porous membrane.* **Kima M., Kiyoharab S.,Konishia S.,Tsunedac S.,Saitoc K.,Sugod T.** 1996, Journal of Membrane Science, Vol. 117, pp. 33-38.

31. *A Structural Definition of Polymer Brushes.* **William J. Brittain, Sergiy Minko.** 2007, Journal of Polymer Science: Part A: Polymer Chemistry, Vol. 45, pp. 3505-3512.

32. *Measuring the Forces that Control Protein Interactions.* **Leckband, Deborah.** 2000, Annual Review of Biophysics and Biomolecular Structure, Vol. 29, pp. 1-26.

33. **Wise S.A, Watters R.L.** Bovine Serum Albumin (7% Solution). Gaithersburg, MD : National Institute of Standards & Technology, 2010. SRM 927d.

34. *A study on the adsorption behavior of protein onto functional microspheres.* **Li S., Jie Hu J.,Liu∗B.** 2005, Journal of Chemical Technology and Biotechnology, Vol. 80, pp. 531–536.

35. **Harris E.L.V., Angal S.** *Protein Purification Methods.* New York : Oxford University Press Inc., 1994. ISBN 0 19 963002 X (hbk).

36. *www.separations.us.tosohbioscience.com.* [Online] 2010. http://www.separations.us.tosohbioscience.com/ServiceSupport/TechSupport/ResourceCenter/PrinciplesofChromatography/IonExchange.

37. *Basis Weight Uniformity Of Lightly Needled Hydroentangled Cotton And Cotton Blend Webs.* **D.V. Parikh, Randall R. Bresee, Navzar D. Sachinvala, Legrand Crook,U. Muenstermann, Alfred Watzl, Don Gillespie.** 2006, Journal of Engineered Fibers and Fabrics, Vol. 1, pp. 47-61.

38. *Polyelectrolyte-mediated Protein Adsorption.*